Accepted Manuscript

Highly Sensitive and Selective Chemiresistor Gas/Vapor Sensors based on Polyaniline Nanocomposite: A comprehensive review

Sadanand Pandey

PII: S2468-2179(16)30163-0

DOI: 10.1016/j.jsamd.2016.10.005

Reference: JSAMD 67

To appear in: *Journal of Science: Advanced Materials and Devices*

Received Date: 17 September 2016

Revised Date: 11 October 2016

Accepted Date: 12 October 2016

Please cite this article as: S. Pandey, Highly Sensitive and Selective Chemiresistor Gas/Vapor Sensors based on Polyaniline Nanocomposite: A comprehensive review, *Journal of Science: Advanced Materials and Devices* (2016), doi: 10.1016/j.jsamd.2016.10.005.

Highly Sensitive and Selective Chemiresistor Gas/Vapor Sensors based on Polyaniline Nanocomposite: A comprehensive review

Sadanand Pandey*[a,b]

[a]*Department of Applied chemistry, University of Johannesburg, P.O. Box 17011, Doornfontien 2028, Johannesburg, Republic of South Africa (RSA)*

[b]*Centre for Nanomaterials Science Research, University of Johannesburg, Republic of South Africa (RSA)*

ABSTRACT

This current review pays particular attention to some current breakthrough develop in the area of gas sensors based on polyaniline (PANI) nanocomposite. Conducting polymers symbolize a paramount class of organic materials with boost the resistivity towards external stimuli. But PANI-based sensor experiences some important disadvantage of poor (reproducibility, selectivity, stability). In order to overcome this restriction PANI was functionalised or incorporated with nanoparticles (NPs) (metallic or bimetallic NPs, metal oxide NPs), carbon compounds (like CNT or graphene, chalcogenides, polymers), in order to overcome this restriction and shows outstanding properties for gas sensing. It has been well forecast that host–guest chemistry combined with the utilization of organic and inorganic analog in nanocomposite results in removing their specific disadvantages due to synergetic/complementary effects, the key to the development of strengthening gas/vapor sensing devices. Herein, author summarize recent advantages in PANI nanocomposite preparation, sensor construction, and sensing properties of various PANI nanocomposites-based gas/vapor sensors, such as NH_3, H_2, HCl, NO_2, H_2S, CO, CO_2, SO_2, LPG, vapor of volatile organic compounds (VOCs) as well as chemical warfare agents (CWAs). The sensing mechanisms pertaining to various gases are also discussed. In conclusion part, some existing problems which may hinder the sensor applications and future prospect of the sensor are also presented.

Keywords: Gas sensors; Polyaniline; Sensitivity; Chemiresistive response; Metal oxide nanoparticles, explosive; Chemical warfare agents.

*Corresponding author. *Tel.: (+27) 11-559-6644, Email address:* sadanand.au@gmail.com, spandey.uj@gmail.com; spandey@uj.ac.za

Highly Sensitive and Selective Chemiresistor Gas/Vapor Sensors based on Polyaniline Nanocomposite: A comprehensive review

ABSTRACT

This current review pays particular attention to some current breakthrough develop in the area of gas sensors based on polyaniline (PANI) nanocomposite. Conducting polymers symbolize a paramount class of organic materials with boost the resistivity towards external stimuli. But PANI-based sensor experiences some important disadvantage of poor (reproducibility, selectivity, stability). In order to overcome this restriction PANI was functionalised or incorporated with nanoparticles (NPs) (metallic or bimetallic NPs, metal oxide NPs), carbon compounds (like CNT or graphene, chalcogenides, polymers), in order to overcome this restriction and shows outstanding properties for gas sensing. It has been well forecast that host–guest chemistry combined with the utilization of organic and inorganic analog in nanocomposite results in removing their specific disadvantages due to synergetic/complementary effects, the key to the development of strengthening gas/vapor sensing devices. Herein, author summarize the recent advantages in PANI nanocomposite preparation, sensor construction, and sensing properties of various PANI nanocomposites-based gas/vapor sensors, such as NH_3, H_2, HCl, NO_2, H_2S, CO, CO_2, SO_2, LPG, vapor of volatile organic compounds (VOCs) as well as chemical warfare agents (CWAs). The sensing mechanisms pertaining to various gases are also discussed. In conclusion part, some existing problems which may hinder the sensor applications and future prospect of the sensor are also presented.

Keywords: Gas sensors; Polyaniline; Sensitivity; Chemiresistive response; Metal oxide nanoparticles; explosive; Chemical warfare agents.

1 Introduction

Quickly expanding ecological pollution has been perceived as a paramount concern, and its monitoring has turned into a prime concern for human wellbeing. Advancement of gas detecting gadget is the earnest requirement for miniaturized, reliable, low-cost, compact electronic sensor procedures for a wide scope of uses, for example, air quality monitoring, medical diagnostics, control of food quality or safety of industrial processes and homemade security system [1-8].

Gas sensors are essentially made up of two types; (i) Gas sensors based on organic conducting polymers and (ii) gas sensors made from inorganic metal oxides. Gas sensors develop using organic conducting polymers, [for example, polyaniline (PANI), poly (3,4-ethylene-dioxythiophene) (PEDOT), polypyrrole (PPy), polythiophenes (PTs) etc.] of coveted functionality and conductivity keep on improving gas detecting performance [9-11]. Although, they are sometimes found to be unstable and show poor sensitivity [12] due to the huge affinity of conducting polymers toward volatile organic compounds (VOCs) and moisture present in the environment. Furthermore, gas sensors produced using inorganic metal oxides, for example, tungsten oxide, zinc oxide, tin oxide, titanium oxide, iron oxide, silicon oxide etc., show enhanced detecting qualities because of changing oxygen stoichiometry and electrically active surface charge [13, 14]. However, these gas sensors work at high temperatures (~300–400°C), regularly prompting to baseline drift and oxidation of analytes [15]. The operation of these devices at elevated temperatures causes gradual changes in the properties of the metal oxide nanostructures. The high-temperature operation can cause fusion of grain boundaries, which can avert the stability of the nanostructure and shorten the lifetime of the sensing device. In addition, the operation of such devices at elevated temperatures requires a distinct temperature controlled complex heating assembly and consumes extra power for heating purposes. Though, it shows high sensitivity, the utilization of such gas sensors for reasonable applications is exceptionally restricted.

Thus complication of organic materials such as low conductivity and poor stability, and inorganic materials such as the operation at high-temperature and sophisticated processability forestall their advantage in gas sensor fabrication. Therefore, the use of nanocomposite of these two divisions of materials may develop in gas sensors with enhancing and effective gas sensing peculiarity and operational at low temperature. In the present article, we are specifically focussing on nanocomposites based on conducting

polymer (PANI) in our present review. PANI a well-known conducting polymer, play a major role in gas sensing applications due to the ease of synthesis and its potential to detect various gases [16]. PANI can exist as two different emeraldine classes of compounds, the insulating emerald base form ($\sigma \sim 10^{-5}$ S/cm) which can be converted into metallic, emeraldine salt conducting form (σ < 1000 S/cm) by protonic acid doping process (Figure. 1) [17–21].

<<Appropriate place for the figure. 1>>

PANI structures such as nanowires (NWs) or nanoparticles (NPs) were suggested to strengthen the response time of the sensor by increasing the surface-to-volume ratio. But PANI-based sensor experiences some important disadvantage of poor (reproducibility, selectivity, stability). In order to overcome this restriction PANI was functionalised or incorporated with nanoparticles (NPs) (metallic or bimetallic NPs, metal oxide NPs), carbon compounds (like CNT or graphene, chalcogenides, polymers), in order to overcome this restriction and shows outstanding properties for gas sensing. From the literature, it was clear that PANI nanocomposite containing inorganic NPs result in enhancement of gas sensitivity [22-24]. It was observed that properties of PANI can be influenced by NPs by two different ways.

In the first place, n-type semiconducting NPs (e.g. WO_3, TiO_2, SnO_2) may bring about the development of p-n heterojunctions at PANI/NPs interfaces [25]. Thus, depletion regions may appear at PANI/ TiO_2 interfaces. Because of the low local density of charge carriers, conductivity in depletion regions is generally poor. At the point, when PANI is influenced by deprotonating gas (e.g. NH_3) a width of depletion regions increase, which increases the sensor response. The second impact of NPs transfers on their catalytic properties. Interaction amongst PANI and specific gas is encouraged by gas particles adsorbed on a NPs surface. Distinctive nanocomposite structures were proposed including catalytic inorganic NPs [25-28]

In a previous couple of years, different types of sensors have been developing using conducting polymers in different transduction modes. They are the potentiometric mode, amperometric mode, colorimetric mode, gravimetric mode and conductometric mode. In the present review, we will consider exclusively the conductometric mode, where the gas detection is through the change of the electrical conductivity, of the conducting polymer. The

change of the electrical conductivity can be because of charge-transfer with the gas molecules or by the mass change due to the physical adsorption of the gas molecules.

This review focuses on PANI-based nanocomposite gas/vapor sensors for environmental monitoring. Figure 2 illustrates the PANI-based nanocomposite used to detect wide range of gas/vapor-sensing applications**.**

<<Appropriate place for the figure. 2>>

2. PANI-based nanocomposite gas/vapor sensors

PANI-based nanocomposite has shown excellent sensing properties toward NH_3, H_2, HCl, NO_2, H_2S, CO, CO_2, SO_2, LPG, and volatile organic compounds (VOCs). Subsequently, some information from related works such as detection limit, sensing range, response time (t_{res})/recovery time (t_{rec}), repeatability, and stability are likewise concisely and carefully was summarized and discussed. Efforts have been made to exploit these sensitivities in the development of new sensor technologies. Table 1 summarise the recent researches about diverse PANI nanocomposites with possible application as gas/vapor sensors.

<<Appropriate place for Table. 1>>

2.1. PANI-based nanocomposite for Ammonia (NH_3) Detection

Ammonia (NH_3) is a colorless gas and water-soluble with a characteristic pungent smell. Inhalation of NH_3 gas for longer time may cause various health related issues such as acute respiratory conditions (laryngitis, tracheobronchitis, bronchiolitis, bronchopneumonia and pulmonary edema), strong irritating effect over our eyes, noses, mouths, lungs and throats, which can further give rise to headache, vomiting, dyspnea, pneumonia-edema and even death [29, 30]. The Occupational Safety and Health Administration (OSHA) have stipulated that the specified threshold limit value for NH_3 in the workplace is 50 ppm. NH_3 is known to be one of the important industrial raw materials used in the production of basic chemicals, textiles, fertilizer, paper products and sewage treatment [31]. In the case of explosives, ammonium nitrate gradually decomposes and releases trace amounts of NH_3, which if detected would be helpful in detection of an explosive. Thus due to the harmful effect of NH_3 related to human health, the environment and use in explosives, stringent action need to be urgently taken in order to monitor the trace level of NH_3.

Recently, a great deal of efforts had presented a great leap forward in the development of PANI nanocomposite based gas sensors for NH_3 detection. Kumar et al. [32] reported NH_3

gas sensor, which was fabricated by using chemically synthesized gold nanostars (AuNS) as catalysts and show that they enhance the sensing activity of insulating PANI thin films. It was observed that the use of AuNS has increased the sensitivity for the same concentration level of NH_3, compared to that for gold nanorods (AuNR) and spherical AuNPs. For 100 ppm NH_3, the sensitivity of the AuNS-PANI composite (AuNS∼170 nm) composites increased to 52%. The AuNS-PANI composite even showed a t_{res} as short as 15 s at room temperature (RT).

Jiang et al. [22] reported the manufacturing of 2D-ordered, large effective surface area, free-standing and patterned nanocomposite platform of PANI nano bowl- AuNPs (15 nm) which was self-assembled onto polystyrene spheres at the aqueous/air interface as a template and utilized for NH_3 detection (0–1600 ppm). The sensor with a thickness of ∼100 nm displayed a quick response time (t_{res}) of 5 s with a recovery time (t_{rec}) of 7 s at 100 ppm of NH_3. Response results were found to be enhanced.

Tai and his team investigated NH_3 gas-sensing behaviors of PANI/TiO_2 nanocomposite synthesized by in-situ chemical oxidation polymerization approach, of which the sensitivity (S) and the recovery time (t_{rec}) were enhanced by the deposition of TiO_2 NPs on the surface of PANI films [33]. The thin film of PANI/TiO_2 nanocomposite reports the improved conductivity contrasted with the pristine PANI film, inferring that an expansion of the conjugation length in PANI chains and the effective charge transfer amongst PANI and TiO_2 may bring about an increment of conductivity. The author presented the response and recovery property of the PANI/TiO_2 sensor for the various concentration of NH_3 (23 to 141 ppm). It can be observed that the resistance of the sensor expanded drastically when to expose to NH_3 analyte, and afterward slowly diminished when NH_3 analyte was replaced via air. It was seen that the response of the sensor at 60 °C diminished contrasted and that deliberate at RT, which might be ascribed to the exothermic adsorption of NH_3 [33]. In most of the cases, sensor response (S) is generally defined as the ratio of the change in resistance (R_g –R_a) upon exposure to target analyte to the resistance (R_a) of the sensor in clean carrier (dry N_2) gas.

$S= (R_g-R_a) / R_a \times 100$ %……………………………………………….(1)

Where, R_g and R_a are the resistances of the sensor in the presence of NH_3 and in a pure carrier gas (dry N_2) respectively.

The typical experimental setup for the analysing chemiresitive gas sensor was shown in Figure. 3. The film of the sensor was placed in a closed glass chamber and the electrical

resistance of the sensor film was measured by a multimeter (Keithley meter) through two conductive needles when analyte gas was injected into the chamber.

<<Appropriate place for the figure. 3>>

Sensor response (S) for PANI/TiO_2 composite based sensors for NH_3 concentration (23 and 117 ppm) was found to be (1.67 %) and (5.55 %) respectively. Response time (t_{res}) is the time required for the sensor to respond to a step concentration change from zero to a certain concentration value. Recovery time (t_{rec}) is the time it takes for the sensor signal to return to its initial value after a step concentration change from a certain value to zero. They reported the t_{res} and t_{rec} time characteristics of PANI/TiO_2 for an exposure of (117 ppm) of NH_3 gas at RT (25°C) were found to be 18 s and 58 s, respectively. It was also observed with exposure of NH_3 (23 ppm) at RT, shows great reproducibility of the sensor. The results also confirm that the response, reproducibility, and stability of the PANI-TiO_2 film to NH_3 is superior to CO gas with a much smaller effect of humidity on the resistance of the PANI/TiO_2 nanocomposite [33]. Chang et al. [34] investigated the fabrication of Gold/PANI/Multiwall carbon nanotube (Au/CNT-PANI) nanocomposite for online monitoring of NH_3 gas. The sensor exhibited a linear detection range from (200 ppb to 10 ppm), a mean sensitivity of 0.638 (at 25 ppm), a t_{res} of 10 min, and a t_{rec} of 15 min [34]. Thus Au/CNT-PANI nanocomposite show superior sensitivity and good repeatability upon repeated exposure to NH_3 gas. The mechanism for sensing of Au/CNT-PANI nanocomposite is determined by the protonation/deprotonation phenomena. As NH_3 gas is injected, NH_3 gas molecules withdraw protons from N^+–H sites to form firmly more favorable NH_4^+. This deprotonation process reduces PANI from the emeraldine salt state to the emeraldine base state, leading to the reduced hole density in the PANI and thus an increased resistance. When the sensor is purged with dry air, the process is reversed, NH_4^+ decomposes to form NH_3 and a proton, and the initial doping level and resistance recover.

Crowley et al. [35] use screen printing and inkjet printing methods in order to fabricate the NanoPANI-modified interdigitated electrode arrays (nanoPANI-IDAs for NH_3 sensing at RT. The sensor was reported to show a stable logarithmic response to an analyte (NH_3) in the concentration of (1–100 ppm). The Sensor response for Inkjet-printed PANI thin films sensors for NH_3 (100 ppm) was found to be 0.24 %. The t_{res} and t_{rec} characteristics of Inkjet-printed PANI thin films for (100 ppm) of NH_3 gas at RT (25°C) were found to be 90 s and 90 s, respectively [35]. Deshpande et al. [36] reported the synthesis of SnO_2/PANI

188 nanocomposites by incorporating SnO_2 particles as colloidal suspensions in PANI through
189 solution route method for detecting NH_3 gas at RT. Schematic diagram of the formation of
190 SnO_2/PANI nanocomposite thin films was shown in (figure 4).

191 **<<Appropriate place for the figure. 4>>**

192 I–V characteristics for pure SnO_2, pure PANI, and the SnO_2/PANI nanocomposites
193 films kept at RT, was shown in (figure 5a, b and c) respectively. It can be clearly observed
194 from (figure. 5a), that no appreciable change was seen in pure SnO_2, while in the case of pure
195 PANI large changes in resistance within a minute on NH_3 gas exposure was observed (figure
196 5b). The I–V attributes of the SnO_2/PANI nanocomposites films demonstrate an alternate
197 however all the more fascinating phenomenon that the SnO_2/PANI nanocomposites films
198 resistance decrease on introduction to NH_3 (~300 ppm) (figure.5c). Moreover, the I–V
199 attributes of SnO_2/PANI nanocomposites reveal a diode-like exponential conduct, which is a
200 characteristic for percolation in disordered systems, wherein the electrical conductance is
201 found to be through hopping mechanism [36]. The sensitivity (S %) of SnO_2/PANI
202 nanocomposites films, on introduction to NH_3 (500 ppm) was observed to be 16. In the event
203 of SnO_2/PANI nanocomposites films, a smooth increment of response was seen up to 300
204 ppm, and it stays same from there on. The SnO_2/PANI nanocomposites films have t_{res} of 12–
205 15 s, and the t_{rec} around 80 s. It might be seen that the SnO_2/PANI nanocomposites films
206 indicated quicker t_{rec} (a variable of 2) when to compare with the PANI films. It was clearly
207 observed that with exposure to NH_3 gas (100–500 ppm in air) at RT, The resistance of PANI
208 film increases, while the film of SnO_2/PANI decreases [36].

209 **<<Appropriate place for the figure. 5>>**

210 Zhang et al. [37] fabricated camphor sulphonic acid (CSA)-doped PANI–SWCNT
211 nanocomposite-based gas sensor (diameter 17–25 nm) using electropolymerization for the
212 selective and sensitive detection of NH_3. The NH_3 sensing performed in the range of 10 ppb
213 to 400 ppm. The sensor response was found to be 50 for 400 ppm of NH_3 at 0% relative
214 humidity (RH). The PANI (CSA)–SWNTs shows greater sensitivity because of an affinity of
215 NH_3 to PANI. The selectivity of the sensor was studied using 1 ppm of NO_2, 3000 ppm of
216 H_2O, and 1 ppm of H_2S. It was observed that PANI (CSA)–SWNTs shows insensitive to at
217 least 1 ppm NO_2, 3000 ppm H_2, and 1 ppm H_2S which confirm high selectivity of PANI
218 (CSA)–SWNTs toward NH_3 sensing [37]. Tai et al. [38] fabricated nanocomposite of PANI
219 with TiO_2, SnO_2, and In_2O_3 using the in situ self-assembly technique for NH_3 sensing

(23−141 ppm). The sensor response of different PANI nanocomposite i.e PANI/TiO_2 (1.5 for 23 ppm and 9 for 141 ppm); PANI/SnO_2 (1.2 for 23 ppm and 7 for 141 ppm) and PANI/In_2O_3 (0.45 for 23 ppm and 1.35 for 141 ppm). The results of sensing studies also showed that all PANI-based nanocomposite systems had the faster t_{res} (2−3 s) and t_{rec} (23−50 s) times with better reproducibility (4 cycles) and long-term stability (30 days) [38]. It has been assumed that p-type PANI and n-type oxide semiconductor may form a p-n junction and a positively charged depletion layer on the surface of inorganic nanoparticles is created. This would cause a lowering of the activation energy and enthalpy of physisorption for NH_3 gas, leading to the higher gas sensing attributes than pure PANI thin film.

Lim et al. [39] researched the electrical and NH_3 gas detecting properties of PANI−SWNTs utilizing temperature-dependent resistance and FET transfer characteristics. The detecting response because of the deprotonation of PANI was observed to be positive for NH_3 (25−200 ppb) and negative to NO_2 and H_2S. This sensitivity of PANI−SWNTs sensor was found to be 5.8% (for NH_3), 1.9% (for NO_2), and 3.6% (for H_2S) with lower detection limits of 50, 500, and 500 ppb, individually [39]. It was also observed that the Sensor response was found to decreased with the increase in the concentration of NH_3 from (75 min at 50 ppb) to (1 min at 100 ppm), while recovery time (t_{rec}) ranged from several minutes to a few hours depending on the concentration. Although the poor selectivity of this fabricated sensor restricts its further application.

Gong et al. [40] prepared a P-type conductive PANI nanograin onto an electrospun n-type semiconductive TiO_2 fiber surface for NH_3 detecting. It can be seen that the increase of NH_3 concentration, the sensitivity greatly increases. The sensitivities of the film were reported to be 0.018, 0.009, and 0.004 for 200, 100, and 50 ppt of NH_3 analyte, respectively. The reproducibility and recovery of the sensor were tested using 10 ppb of NH_3 for 5 cycles [40]. Pawar et al. [41] demonstrated the fabrication of PANI/TiO_2 nanocomposite for selective detection of NH_3. This nanocomposite sensor is found to exhibit gas response towards an NH_3 concentration up till 20 ppm. The NH_3 detection range is from 20 ppm to 100 ppm. Sensor response for PANI/TiO_2 nanocomposite sensor for NH_3 (20 ppm and 100 ppm) was found to be 12 and 48 %. The t_{res} and t_{rec} for films sensors for an exposure of (20 ppm and 100 ppm) of NH_3 gas at RT (25°C) were found to be (72 s, 340 s) and (41 s, 520 s), respectively. It was suggested that the response was owing to the creation of a positively charged depletion layer at the heterojunction of PANI and TiO_2 [41]. Wojkiewicz et al. [42] reported the NH_3 sensing in the range of ppb from fabricated Core-shell nanostructures

PANI-based composites. The NH_3 detection range is from 20 ppb to 10 ppm. Sensor response for Core-shell PANI thin films sensors for NH_3 (1ppm) was found to be 0.11%. The t_{res} and t_{rec} of Inkjet-printed PANI sensors for an exposure of (1 ppm) of ammonia gas at RT (25°C) was found to be 2.5 min and 5 min, respectively [42].

Patil et al. [43] demonstrated the performance PANI-ZnO nanocomposite for NH_3 sensing at RT. The surface morphology of nanocomposite by utilizing SEM method demonstrates the uniform distribution of the ZnO NPs and no agglomeration in the PANI framework. It was viewed as that the nanostructured ZnO NPs encompassed inside the mesh-like structure built by PANI chains. It was observed that morphology assumes a critical part in sensitivity of the gas detecting films [43]. The grain sizes, structural formation, surface to volume proportion and film thickness are essential parameters for gas detecting films. The PANI-ZnO (50%) nanocomposite gives the superb gas response contrasted with whatever is left of composites additionally these films demonstrated improved stability, reproducibility, and mechanical strength because of ZnO NPs in the PANI films. It is observed that thin films can sense a lower concentration of NH_3 (20 ppm) with higher sensitivity (~ 4.6) when contrasted with large concentration (100 ppm) of different gasses (CH_3OH, C_2H_5OH, NO_2, and H_2S). The expansion in resistance after introduction to NH_3 might be a direct result of the porous structure of PANI-ZnO films prompts the prevalence of surface phenomena over bulk material phenomena, which may again be because of surface adsorption impact and chemisorptions prompt the formation of ammonium. It was seen that the reaction time (t_{res}) and recovery time (t_{rec}) fluctuates inversely with respect to the concentration of NH_3. The response time (t_{res}) diminishes from (153 s to 81 s) while recovery time (t_{rec}) increments from (135 to 315 s) with expanding NH_3 concentration from (20 to 100 ppm) [43]. The decrease accordingly time might be because of extensive availability of vacant sites on thin films for gas adsorption as obvious from SEM picture, and expanding recovery time might be because of gas reaction species which deserted after gas interaction bringing about the decrease in desorption rate [43].

Venditti et al. [44] fabricated the nanoPANI–Au composite utilizing PANI and AuNPs functionalized with 3-mercapto-1-propanesulfonate by an osmosis based technique (OBM) keeping in mind the end goal to improve the effective surface area. It was observed that when AuNPs have been assembled with PANI in the OBM strategy, by utilizing dimethylformamide (DMF) as the solvent, spherical polymeric NPs with fused AuNPs have been collected affirm from SEM technique. Sensor performance of undoped nanoPANI and

nanoPANI–Au was concentrated on to improve the responses to various analytes (NH_3 vapors, water, acetonitrile, toluene, and ethanol) by resistive measurements at RT. It was observed that nanoPANI–Au demonstrates an improved response w.r.t nanoPANI. If there should be an occurrence of nanoPANI–Au current intensity increments from 25×10^{-12} to 1×10^{-9}A on fluctuating the RH from (0 to 70%). After H_2SO_4 doping, nanoPANI–Au tests demonstrate a superior response to NH_3 vapor (10.8 ppm) at RT with outstanding selectivity and sensitivity 1.9% ppm^{-1} [44]. PANI nanocomposite films inserted TiO_2 NPs synthesis by electrochemical polymerization of aniline (ANI) with TiO_2 NPs added into the solution for NH_3 detecting was demonstrated by Kunzo et al. [45]. It was additionally reported that the nanocomposite detecting film morphology and electrical resistivity were controlled by voltammetric parameters and ANI concentration. FTIR spectra of nanocomposite confirm the presence of chemical bonding between the NPs and polymer chains. The films were tried for sensitivity to NH_3. It was observed that because of TiO_2 NPs, the sensitivity of the composite film expanded two times achieving a 500% change in resistance at the use of 100 ppm of NH_3 [45].

Wu et al. [46] fabricated the graphene/PANI nanocomposites as conductometric sensors for the detection of NH_3. It was observed that graphene/PANI-based sensor increases the resistance with exposure to different NH_3 concentration (1-6400ppm). The indication of the higher sensitivity of the sensor can easily be proof based on 1ppm of NH_3 detection. The sensor response values of graphene/PANI and PANI sensors were found to exhibit linearity for NH_3 concentrations (1 to 6400 ppm). Sensor response for graphene/PANI thin films sensors for NH_3 concentration (20 and 100 ppm) was found to be 3.65 and 11.33 % respectively. The t_{res} and t_{rec} characteristics of graphene/PANI thin films sensor for an exposure of (100 ppm) of NH_3 gas at RT (25°C) were found to be 50 s and 23 s, respectively. In respect to PANI film, graphene/PANI sensor exhibit much faster response and shows excellent reproducibility for NH_3 gas [46]. Zhang and co-workers reported the high sensitivity of PANI/PMMA nanocomposite for the detection of NH_3 (1 ppm) [47]. The reason for trace detection can be because of PANI coating onto highly aligned PMMA microfibers, which result in faster diffusion of gas molecules, through accelerating electron transfer [47].

Abdulla et al. [48] reported the trace detection of ammonia by using PANI/MWCNTs sensor. The author used in-situ oxidative polymerization method for the synthesis of PANI/MWCNTs sensor by utilizing ammonium persulfate (APS) as an oxidizing agent. The

procedure followed for the fabrication of sensing material was provided in (figure 6). PANI/MWCNTs synthesis involve following steps: First, acid treatment of MWCNTs was performed in order to de-bundling of CNTs due to the formation of –OH and –COOH groups on its surface to form carboxylated MWCNTs . Then carboxylated MWCNTs along with ANI monomer by in-situ oxidative polymerization method result in the formation of PANI/MWCNTs nanocomposite. The application in gas sensing of C-MWCNT and PANI/MWCNT based sensors was analyzed by using the changes in the resistance of the sensor upon adsorption of NH_3 gas molecules at RT [48].

<<Appropriate place for the figure. 6>>

The t_{res} and t_{rec} characteristics of C-MWCNTs based sensors for an exposure of (2-10 ppm) of NH_3 gas at RT were found to be (965-1865 s) and (1440-2411 s), respectively. In the case of PANI/MWCNT nanocomposite t_{res} and t_{rec} was found to be (6-24 s) and (35-62 s) respectively. This clearly depicts that PANI/MWCNT nanocomposite shows very fast response and recovery time for NH_3. Sensor response for C-MWCNTs and PANI/MWCNT composite based sensors for NH_3 concentration (2-10 ppm) was found to be (2.58-7.2 %) and (15.5-32 %) respectively [48]. Authors explain the enhancement of sensing performance of PANI/MWCNTs can be related to the combined effect of doping/dedoping of PANI and the electron transfer between the NH_3 molecules and MWCNT. PANI/MWCNTs sensors show good reproducibility and reversibility after 5 cycles of repeated exposure and desorption of NH_3 gas for 2 ppm NH_3 gas. The sensor was found to be highly selective towards NH_3 (15.5% for 2 ppm of NH_3) among the other oxidizing/reducing gasses i.e H_2S (2%), Acetone (5%), Isoprene (5.3%), Ethanol (5.6%) and NO_2 (4%). The fabrication of cellulose/TiO_2/PANI composite nanofiber for sensing of NH_3 at RT was performed by Pang et al. [49]. Figure.7 shows the SEM images of cellulose nanofibers (fig.7a), cellulose/TiO_2 (fig.7b), cellulose/PANI (fig.7c) and cellulose/TiO_2/PANI composite nanofibers (fig.7d). It was observed that cellulose/TiO_2 is less smooth as compared with cellulose. While in the case of cellulose/TiO_2/PANI composite nanofibers, the much roughness on the surface (because of PANI) along with good fibre structure is observed. The present of fibres structure enhances the surface area of cellulose/TiO_2/PANI composite nanofibers which results in easy diffusion of ammonia vapor. In their study, author has done sensing on cellulose/TiO_2/PANI and cellulose/PANI composite nanofibers for NH_3 vapor concentration (10-250ppm) at RT. The response value of cellulose/TiO_2/PANI composite nanofibers was much higher than that of cellulose/PANI composite nanofibers. Sensor response for graphene/PANI thin films sensors

for NH_3 concentration (10-250 ppm) was found to be 0.58-6.3% respectively. The cellulose/TiO_2/PANI sensor exhibit high selectivity (6.33% for 250 ppm of NH_3) among the other gasses such as acetone, ethanol and methanol [49]. It was observed that PANI is a p-type semiconductor, and TiO_2 is n-type, during polymerization of ANI was operated with the cellulose/TiO_2 composite nanofibers as templates, there would be P–N heterojunction formed at the interface between PANI and TiO_2 NPs. So the P–N heterojunction may play an important role in the improvement of gas sensing properties of the cellulose/TiO_2/PANI composite sensors. Thus when exposed to ammonia, the resistance of cellulose/TiO_2/PANI composite nanofibers would increase not only because of the de-doping process but also the change in the depletion layer thickness of P–N heterojunction.

<<Appropriate place for the figure. 7>>

Guo et al. [50] fabricated a hierarchically nanostructured graphene–PANI (PPANI/rGO-FPANI) nanocomposite for detection of NH_3 gas concentrations (100 ppb to 100 ppm), dependable reliable transparency (90.3% at 550 nm) for the PPANI/rGO-FPANI nanocomposite film (6 h sample), fast response t_{res}/t_{rec} (36 s/18 s), and strong flexibility without an undeniable performance decrease after 1000 bending/extending cycles. It was watched that amazing detecting performance of sensor could most likely be attributed to the synergetic impacts and the moderately high surface area (47.896 m^2g^{-1}) of the PPANI/rGO-FPANI nanocomposite film, the productive artificial neural system detecting channels, and the adequately uncovered dynamic surfaces [50]. Zhihu et al. [51] investigated the NH_3 sensing at RT by using porous thin film composites of PANI/sulfonated nickel phthalocyanine (PANI/NiTSPc) were deposited across the gaps of interdigitated Au electrodes (IAE) by an electrochemical polymerization method. The sensor response of the PANI/NiTSPc film to 100 ppm NH_3 was found to be 2.75 with a short t_{res} of 10 s. PANI/NiTSPc film sensor have significant properties of fast recovery rate, good reproducibility and acceptable long-term stability in the range from (5 to 2500 ppm). The outstanding sensing performance of the PANI/NiTSPc composites may be attributed to the porous, ultra-thin film structure [52, 53] and the "NH_3-capture" effect of the flickering NiTSPc molecules.

Khuspe et al. [54] reported NH_3 sensing by using (PANI)-SnO_2 nanohybrid-based thin films doped with 10–50 wt % camphor sulfonic acids (CSA) were deposited on the glass substrates using spin coating technique. FESEM of PANI, PANiSnO_2 (50%) and PANi-

SnO_2-CSA (30%) nanohybrid films at 100K magnification. The Film of PANI has a fibrous morphology with high porosity. PANi-SnO_2 (50%) nanocomposite shows the uniform distribution of SnO_2 nanoparticles in the PANI matrix. The doping of CSA has the strong effect on the PANI-SnO_2 nanocomposites morphology. The nanocomposite shows the transformation in morphology from fussy fibrous into clusters with an increase in CSA content in case of PANI-SnO_2-CSA (30%) nanohybrid. It is observed that PANI-SnO_2 hybrid sensor showed the maximum response of 72% to 100 ppm NH_3 gas operating at RT. A significant sensitivity (91%) and fast response (46 s) toward 100 ppm NH_3 operating at room temperature is observed for the 30 wt % CSA doped PANiSnO_2 nanohybrid film The sensitivity of PANi-SnO_2-CSA (10%), PANi-SnO_2-CSA (20%), PANi-SnO_2-CSA (30%), PANi-SnO_2-CSA (40%), PANi-SnO_2-CSA (50%) nanohybrids to 100 ppm of NH_3 gas were 80%, 86%, 91%, 84% and 75%, respectively, operating at RT.

Tai et al. [55] reported P–P isotype heterojunction sensor was developed by modifying microstructure silicon array (MSSA) with self-assembled PANI nano-thin film for NH_3 detection at RT. It exhibited the high response, good reversibility, repeatability and selectivity when exposed to NH3. The sensor response (S), t_{res} and t_{rec} of sensor is as about 0.8%, 25 s and 360 s to 20 ppm NH_3 at 25°C, respectively. The sensor response was found to be 0.8-1.7% from concentration range of 10-90 ppm of NH_3. Yoo et al. [56] investigated the effects of O_2 plasma treatment on NH_3 gas sensing characteristics (e.g. linearity, sensitivity, and humidity dependence) of pf-MWCNT/PANI composite films. The sensor response, t_{res} and t_{rec} of sensor is as about 0.015%, 100 s and 700 s to 20 ppm NH_3 at 25°C, respectively. The sensor response was found to be 0.01-0.075% from concentration range of 0-100 ppm of NH_3.These results indicate that oxygen-containing defects on the plasma-treated MWCNTs play a crucial role in determining the response of the pf-MWCNT/PANI composite film to NH_3.

Huang et al. [57] studied the NH_3 sensing by using chemically reduced graphene oxide (CRG). Aniline was used to reduce graphene oxide (GO) in order to obtain CRGs attached with different states of PANI, i.e. acid-doped PANI attached CRG, de-doped PANI attached CRG and free CRG. The results clearly suggest that free CRG exhibited an excellent response to NH_3 and showed high sensitivity to NH_3 with the concentrations at parts-per-million (ppm) level. The sensors based on free CRG exhibited a response of 37.1% when exposure to 50 ppm of NH_3 room temperature (25◦C). The sensor also shows high reproducibility and great selectivity. The fabrication of room temperature flexible NH_3 sensor

based on S and N co-doped graphene quantum dots (S, N: GQDs)/PANI) hybrid loading on flexible polyethylene terephthalate (PETP) thin film by chemical oxidative polymerization method was investigated by Gavgani et al. [58]. The S and N co-doped graphene quantum dots (S, N: GQDs) were synthesized by hydrothermal process of citric acid and thiourea. The synthesis of S, N: GQDs and S, N: GQDs/PANI hybrid are schematically shown in figure. 8a and figure.8b respectively. In this study, S, N: GQDs/PANI water solution was drop casted over the PET film (1 cm × 1 cm). The solution was evaporated using vacuum oven at 80°C for 1 h, interdigitated Au electrodes with 400 µm interdigit spacing, 100 nm thickness and 100 µm wide were deposited on a flexible PET substrate by physical vapor deposition method. Finally, the flexible hybrid gas sensor was baked for 1 h in a furnace at 80°C in a N_2 atmosphere. The detail fabricated process of S, N: GQDs/PANI hybrid gas sensor is displayed in Figure. 8b. The sensing response clearly depicts that S, N: GQDs/PANI hybrids have 5 times more sensor response as compare with PANI at NH_3 (100ppm). The conductivities of hybrid and PANI at 10 nA applied current are 32.8 S cm^{-1} and 95.8 S cm^{-1}, respectively. It corresponds to a significant increase of charge carrier concentration due to S,N: GQDs incorporation. Thus, S, N: GQDs plays a dominant role in the charge transport through the PANI matrix. The t_{res} and t_{rec} of flexible pure PANI and S, N: GQDs/PANI gas sensor to 10 ppm of NH_3 are (183 s, 77 s), and (115 s, 44 s), respectively. The sensor response of flexible pure PANI and S, N: GQDs/PANI hybrid gas sensors are 10.1% and 42%, respectively at 100 ppm NH_3. The detection limit of NH_3 gas for flexible pure PANI, and S, N: GQDs/PANI hybrid gas sensors are 1 ppm and 500 ppb, respectively at 25°C in 57% relative humidity (RH). The GQDs/PANI hybrid shows high selectivity. It was observed that sensor response of 100 ppm of NH_3, toluene, methanol, acetone, ethanol, chlorobenzene, and propanol is 42.3, 0.5, 0.45, 0.5, 0.48, 0.51, and 0.48%, respectively. Thus the results show flexible S, N: GQDs/PANI hybrid gas sensor shows very high response to NH_3 but is almost insensitive to other VOC gases.

<<Appropriate place for the figure. 8>>

2.2. PANI-based nanocomposite for Hydrogen (H_2) Detection

Hydrogen is odorless, colorless, and tasteless gas, which is extremely explosive in an extensive range of concentration (4–75%) [59, 60]. Hydrogen is utilized broadly as a part of scientific research and industry as the fuel for the internal combustion engines, rocket propellant, glass and steel manufacturing, shielding gas in atomic hydrogen welding, and

rotor coolant in electrical generators, [61]. The main dangers associated with H_2 gas include high permeability through many materials and flammability. Therefore, development of rapid, accurate, and highly sensitive hydrogen sensors to detect a leakage for safe storage, delivery, and utilization of hydrogen is exceedingly attractive so as to accomplish safe and effective processing of hydrogen on enormous scale. Sadek et al. [62] reported the chemical polymerization technique for fabrication of PANI/WO_3 nanocomposite on the surface of a layered ZnO/64◦ YX $LiNbO_3$ substrate for monitoring of H_2 gas. The experimental process involves exposure of sensor with H_2 gas pulse sequence of (0.06%, 0.12%, 0.25%, 0.50%, 1%, and 0.12%) in synthetic air at RT. It was observed that sensor response was approx. 7 kHz for (1% of H_2) in synthetic air. The 90% t_{res} of 40 s and t_{rec} of 100 s with good reproducibility were observed at RT. It was found that the PANI/WO_3 nanocomposite sensor produces repeatable responses of the same magnitude with good baseline stability [62]. Authors have proposed two possible mechanisms for H_2 sensing. The first mechanism involves the activation of the H_2 molecule by WO_3 due to the formation of tungsten–dihydrogen complexes. While the second possible mechanism can be due to the closer packing of PANI backbones by WO_3, and thus dissociation of the H_2 molecule is stimulated by interaction with a free spin on adjacent PANI chains.

Al-Mashat et al. [63] fabricated the H_2 gas sensor by using graphene/PANI nanocomposite. In the synthesis chemical route was followed for graphene synthesis; follow by ultra-sonication with a blend of ANI monomer in presence of APS (initiator) in order to form PANI on its surface. The SEM microgram result clearly depicts that composite has a nano-fibrillar morphology. Authors have found that the graphene/PANI nanocomposite-based gadget sensitivity is 16.57% toward 1% of H_2 gas, which is much higher than the sensitivities of sensors in view of just graphene sheets and PANI nanofibers.

Nasirian & Moghaddam reported the synthesis of PANI (emeraldine)/anatase TiO_2 nanocomposite by a chemical oxidative polymerization [64]. The thin films of PANI (emeraldine)/anatase TiO_2 nanocomposite for H_2 gas detecting application were deposited on Cu-interdigitated electrodes by spin coating technique at RT. The reaction and t_{res}/t_{rec} time of sensors for H_2 gas were assessed by the change of TiO_2 wt% at natural conditions. Resistance-detecting estimation was displayed a high sensitivity around 1.63, a great long-term response, low response time and recovery time around 83 s and 130 s, individually, at 0.8 vol% H_2 gas for PANI(emeraldine)/anatase TiO_2 nanocomposite including 25% wt of anatase NPs [64].

Sharma et al. [65] fabricated Al-SnO_2/PANI composite nanofibers via electrospinning technique for H_2 sensing. It can be clearly observed by experimental results that 1% Al-SnO_2/PANI nanofibers have a better response for sensing of hydrogen as compared to that of 1% Al-SnO_2 alone. The results depict that 1% Al-SnO_2/PANI hybrid have high sensitivity (~275%) to H_2 gas (1000 ppm) at 48˚C with relatively faster t_{res} (2 s) and t_{rec} (2 s). Srivastava et al. [66] development of interdigited electrode (IDE) based chemiresistor type gas sensor and the thin films of PANI and CNT-doped PANI for H_2 gas sensing at RT. The gas sensing measurements were performed towards 2% of hydrogen concentration in air at 1.3 atm hydrogen pressure at RT. The response of PANI film is observed around 1.03, which increases up to 1.06 and 1.07 for MWNT/PANI and SWNT/PANI composite films respectively. In the case of SWNT/PANI and MWNT/PANI composite films, the conducting paths are formed due to quantum mechanical tunneling effects and electron hopping can occur through conducting channels of CNT. The presence of SWNT and MWNT in PANI may promote the possibility of more H_2 absorption due to their centrally hollow core structure and their large surface area provide more interaction sites within PANI composite that are available for H_2 sensing.

Srivastava et al. [67] reported the effect of Swift heavy ion (SHI) irradiation on the gas sensing properties of tantalum (Ta)/PANI composite thin film based chemiresistor type gas sensor for H_2 gas sensing application at RT. It was observed that unirradiated Ta/PANI composite sensor shows negligible response. It may be due to the Ta layer coated over the PANI surface, which does not react with H_2 at RT and inhibited the hydrogen to diffuse into the PANI matrix. Therefore at RT pristine Ta/PANI sensor dose not shows any response for H_2. While upon irradiation, it was observed that Ta/PANI composite sensor show a higher response and the response increases slightly with increasing ion fluence. The response value has been found ~1.1 (i.e. % Sensitivity ~9.2%) for Ta/PANI composite sensor irradiated at fluence 1 x 10^9 ion/cm^2, which was increased up to 1.42 (i.e. % Sensitivity ~ 30%) for composite sensor irradiated at fluence 1 x 10^{11} ion/cm^2 (Figure.9). It may suggest that due to the SHI irradiation Ta melts and diffuses into PANI matrix, which provides comparatively rough, and higher surface area for hydrogen adsorption and rapid diffusion, therefore more interaction sites are available for hydrogen sensing and hence the sensing response is increased. It has been reported that rough and fiber-like structure of PANI shows a faster and higher response for hydrogen than conventional PANI film, because the three-dimensional

porous structure of a PANI nanofibers allows for easy and rapid diffusion of hydrogen gas into PANI [68,69].

<<Appropriate place for the figure. 9>>

Nasirian et al. [70] investigated the gas sensing at 27°C by using PANI/TiO_2:SnO_2 nanocomposite deposited onto an epoxy glass substrate with Cu-interdigited. The schematic diagram of our handmade gas sensor setup was shown in figure.10. The typical structure of H_2 sensor consists of a layer of PTS on a finger type Cu-interdigited electrodes patterned area of an epoxy glass substrate and two electrodes. The sensor response (S), response (t_{res}) and recovery time (t_{rec}) calculation is the same ways as it explain earlier. H_2 gas sensing results demonstrated that a PTS sensor with 20 and 10 wt % of anatase-TiO_2 and SnO_2 NPs, respectively, has the best t_{res} (75 s) with a t_{rec} of 117 s and have sensitivity of 1.25 (0.8 vol% H_2). The human development has been grouped by paramount material on which the modern innovation is based like Stone Age, Iron Age and now the Polymer Age [71]. This age is properly called the polymer age because of broad utilization of polymers in all domains of life [72-93]. Li et al. [94] reported high sensitivity and high selectivity, and response towards H_2 gas using chitosan (biopolymer) in Chitosan/PANI composite at RT. The Chitosan/PANI composite and pure PANI structures in response to 4% H_2 gas diluted in air at RT shows following results. Firstly resistance increased with the Chitosan/PANI composite while it decreased with the pure PANI upon exposure; secondly response with the Chitosan/PANI composite film was higher (at~130%) than with the PANI at~28%; The sensor response to the H_2 gas concentration ranging from 0.3 to 4% was found to be quite linear.

<<Appropriate place for the figure. 10>>

2.3. PANI-based nanocomposite for Hydrochloric Acid (HCl) Detection

Hydrochloric acid (HCl) occurs as a colorless, non-flammable aqueous solution or gas. HCl is mostly used in different industrial sectors; it is extremely dangerous for both living beings and the environment. It was observed that exposure to concentrated HCl may even be fatal because of circulatory collapse or asphyxia caused by glottic oedema [95]. Low concentrations of HCl solutions exposure may causes different health problems such as conjunctivitis, corneal burns, ulceration of the respiratory tract, dermatitis, skin burns, bronchitis, pulmonary oedema, dental erosion, hoarseness, nausea, vomiting, abdominal pain, diarrhoea, permanent visual damage etc. [95, 96]. The airborne permissible exposure limit (PEL) for HCl is 5 ppm in 8 hour work day. A concentration of 100 ppm is known to be

immediately dangerous to life or health (IDLH) [97]. Thus there is need for HCl sensors.. Mishra et al. [98] fabricated a specific, quick and sensitive HCl gas sensor by utilizing nanocomposites of copolymers of ANI and HCHO prepared with a metal complex of Fe−Al (95:05) by means of thermal vacuum evaporation deposition techniques. This sensor detects HCl (0.2 to 20 ppm) in 8−10 s. These nanocrystalline composite film displayed high sensitivity (400−800) and a t_{res} of 10 s. The selectivity was accomplished by appropriate doping of PANI during synthesis. The sensor was reusable, as there was no chemical reaction between PANI film and HCl gas. Moreover, the sensor worked at RT and had a broadened lifetime.

2.4. PANI-based nanocomposite for nitrogen oxides (NOx) Detection

Nitrogen oxides include the gases nitrogen oxide (NO) and nitrogen dioxide (NO_2). NO_2 forms from ground-level emissions results of the burning of fossil fuels from vehicles, power plants, industrial sources, and off-road equipment. NO_2 cause harmful effects on human health and the environment. Exposure of NO_2 causes several respiratory system problems in human being. On January 22, 2010, EPA strengthened the health based National Ambient Air Quality Standard (NAAQS) for NO_2. EPA set a 1-hour NO_2 standard at the level of 100 ppb. EPA also retained the annual average NO_2 standard of 53 ppb. Yun et al. [99] investigated the sensing of NO by fabricating PANI/MWCNT/TiO_2 composite using in situ polymerization method. The electrical resistance decreased upon NO gas exposure which is the typical characteristics of a p-type semiconductor. The decrease in the electrical resistance is attributed to the electron charge transfer between NO gas and the surface of PANI/MWCNT p-type semiconductors. PANI/MWCNT/TiO_2 composite sensor shows the highest sensitivity of 23.5% to NO (25 ppm) at 22 °C. The sensor showed excellent reproducibility in gas sensing behaviour during the recovery process at lower temperature of 100°C.

Xu et al. [100] demonstrated the NO_2 sensing by using SnO_2–ZnO/PANI composite thick film. The SnO_2–ZnO/PANI composite was fabricated from SnO_2–ZnO porous nano solid and PANI by a conventional coating method. The SnO_2–ZnO composite porous nanosolid was synthesized by a solvo-thermal hot-press technique. It was observed that sensor based on SnO_2–ZnO/PANI composite sensor showed high stability to NO_2 (35 ppm) monitored for 22 min at 180°C. The sensor response to 35 ppm NO_2 increases from (40 to 180 °C) and start decreases after further increasing temperature. SnO_2–ZnO (20 wt %)/PANI composite sensor has the highest sensor response (S%) of 368.9 at 180 °C. Selectivity study

of the sensor was also performed at 180°C by using different analytes (NO_2, NH_3, H_2, C_2H_5OH, and CO). It was observed that sensor response of analytes (NH_3, H_2, C_2H_5OH, and CO) was below 3%, while of NO_2 was found too high sensor response of 368.9. The results depict that sensor SnO_2–ZnO (20 wt %)/PANI composite have high sensitivity (368.9%) to NO_2 (35ppm) at 180 °C with relatively faster t_{res} (9 s) and t_{rec} (27 s).

WO_3–PANI and hemin/ZnO-PPy nanocomposite thin film sensors were prepared by Kaushik et al. [101] and Prakash et al. [102] respectively, to detect NOx gasses. The NOx gas sensing characteristics of the sensors were performed by measuring the change in resistance w.r.t time. This sensor exhibited a linear range of 0.8–2000 μM, a sensitivity of 0.04 μM^{-1} and a detection limit of 0.8 μM at RT. Sharma et al. [103] showed the gas detecting properties of (0.5–3% PANI)-SnO_2 sensors for trace NO_2 gas detection. It was accounted for that (1% PANI)-SnO_2 sensor film indicated high sensitivity towards NO_2 gas alongside a sensitivity of 3.01×10^2 at 40°C for 10 ppm of gas. On introduction of NO_2 gas, the resistance of all sensors expanded to a substantial degree, considerably more prominent than three orders of magnitude. After removal of NO_2 gas, changes in resistance are observed to be reversible in nature and the fabricated composite film sensors demonstrated great sensitivity with moderately quicker t_{res}/t_{rec} [103].

The NO_2 detection by using SnO_2/PANI double-layered film sensor fabricated using nanoporous SnO_2 and PANI layers by Xu et al. [104]. Double layered film sensor shows high selectivity and high response to NO_2 gas even with low concentration. The sensor response, tres and trec time of sensor S5P500 is as short as about 4%, 17 s and 25 s to 37 ppm NO_2 at 140°C, respectively. The sensor response was found to be 1-13% from concentration range of 5-55 ppm of NO_2. Selectivity of the sensor was studied using following gases; 1000 ppm CO, 1000 ppm H_2, 1000 ppm, C_2H_5OH vapor, 10 ppm NO_2 and 10 ppm NH_3. It was observed that sensor S5P100 had a comparatively strong response to 10 ppm NO_2, but no response to other gases was observed when the working temperature was lower than 180°C. Reproducibility of two sensor S5P100 & S5P500 to 37 ppm of NO_2 at 140°C was performed. The sensors show high reproducibility up till four cycles (Figure.11). The mechanism for improvement in NO_2 sensing may be due to the formation of the depletion layer at the p–n junction interface in SnO_2/PANI double layered film sensor, which makes great resistivity difference in air and NO_2 gas.

<<Appropriate place for the figure. 11>>

2.5. PANI-based nanocomposite for Hydrogen Disulfide (H_2S) Detection

Hydrogen sulfide (H_2S) is a colorless, flammable, extremely hazardous gas. It occurs naturally in crude petroleum, natural gas, and hot springs. Exposure to low concentrations of H_2S causes irritation in the eyes, nose, throat and respiratory system (e.g., burning/ tearing of eyes, cough, shortness of breath). High concentrations of H_2S can cause shock, convulsions, inability to breathe, extremely rapid unconsciousness, coma and death. The OSHA has stipulated that the specified threshold limit value for H_2S in the workplace is 20 ppm. A level of H_2S gas at or above 100 ppm is IDLH. Thus monitoring of H_2S is very important. Shirsat et al. [105] reported the PANI nanowires bridging the 3 μm gap between two Au IDEs were synthesized using a two-step galvanostatic electrochemical polymerization technique. Nanowire networks were further functionalized by controlled growth of AuNPs of size ~70−120 nm. PANI/Au nanocomposite exhibited an outstanding response to H_2S gas (~0.1 ppb) with good selectivity and reproducibility [105]. Authors have proposed a plausible mechanism for the formation of AuS [Eqn (2)] and subsequent protonation of PANI for H_2S detection by PANI/Au nanocomposites.

$$H_2S+Au \rightarrow AuS+2H^+ \quad \text{.....(2)}$$

The authors suggested that transfer of electrons from PANI to Au led to a drop in resistance of the material.

Crowley and coworkers, developed PANI/$CuCl_2$ sensor printed on screen printed interdigitated electrodes for trace level H_2S detection. H_2S exerted an oxidizing effect on PANI due to preferential binding of $CuCl_2$ with S^{2-} ion with the evolution of HCl, which protonated PANI increasing its electrical conductivity [106]. Raut and his co-workers reported a fabricated the CSA-doped PANI-CdS nanocomposite synthesis by using chemical polymerization for the selective detection of H_2S (10−100 ppm) [107]. This sensor exhibited a maximum response of 76% at 100 ppm and 97.34% stability after 10 days for 40% doping of CSA in the PANI-CdS nanocomposite. The CSA-PANI-CdS sensor exhibited negligible response (2−5%) to NO_2, CH_3OH, C_2H_5OH, and NH_3. Unfortunately, however, this sensor possesses a high recovery time of ~205−413 s.

Raut,et al. [108] investigated H_2S sensor based on PANI–CdS nanocomposites fabricated by a simple spin coating technique at RT (300 K). The resistance of PANI–CdS nanocomposites showed a considerable change when exposed to various concentrations of H_2S. The sensor response of ~48% was achieved for 100 ppm H_2S for PANI–CdS

nanocomposites sensor. Based on the concentration of H_2S, the t_{res} and t_{rec} was found to be in the range of (41-71 s) & (345–518 s) respectively. It can be clearly observed in the figure.12, that PANI–CdS nanocomposite films can sense the lower concentration of H_2S with higher sensitivity value as compared to the large concentration of other gases. The plausible mechanism of selectivity for H_2S may be traced to the characteristics of vapor adsorbed over the surface of PANI–CdS nanocomposites.

<<Appropriate place for the figure. 12>>

Mekki et al. [109] fabricated flexible PANI–Ag nanocomposite films on (3-aminopropyl) trimethoxysilane (APTMS) modified biaxially oriented polyethylene terephthalate (BOPET) by in situ effortless UV prompted polymerization of ANI in the presence of $AgNO_3$. Low magnification SEM picture PANI–Ag films (arranged with $AgNO_3$ 0.5 M), demonstrates the nano-brush morphology. I–V curves for these films are straight demonstrating an ohmic contact between Au electrode and PANI–Ag films. The chemiresistive gas detecting properties of PANI–Ag films were researched by the presentation of 10 ppm of every test gasses, for example, NH_3, H_2S, Cl_2, NO, NO_2, CO, CH_4, and C_2H_5OH. Among all gasses PANI–Ag films demonstrated the response for H_2S only. The expansion in current on presentation to H_2S (1–25 ppm) was observed [109]. The gas detecting results, (for example, lowest detection limit (LDL) of 1 ppm with a high response 100% and quick response time 6 min at 10 ppm) was acquired. The mechanism for the interaction of H_2S with PANI-based composites can be clarified by dissociation of H_2S on the metal surface under surrounding condition since it is a weak acid (acid dissociation constant pKa = 7.05). The dissociation of H_2S results into H^+ and HS^- ions. The subsequent HS^- anion makes up for the positive N^+ charges in the PANI chains, however, there is additionally proton liberation in the films. Since the mobility of cation (H^+) is much bigger than the anion (HS^-), in this manner the general impact is the slight conductance ascend on presentation to H_2S.

2.6. PANI-based nanocomposite for Volatile Organic Compounds (VOCs) Detection

Volatile organic compounds (VOCs) are a standout amongst the most mainstream gases whose detections are exceedingly attractive. There is, therefore, a surge of enthusiasm for the development of VOCs sensors in light of the fact that they continually risk our well-being as well as the environment around us and cause chronic health threats to human beings, animals and plants. Volatile organic compounds also contribute to climate change and destruction of

the ozone layer [110, 111]. The low flashpoints of VOCs make them particularly threatening in closed areas. Thus, there is increased demand for the development of a continuous real-time technique to monitor VOCs.

$CHCl_3$ vapors depress the central nervous system (CNS) of human beings and animal. Chronic chloroform exposure can damage the liver, kidneys, and develop sores when the skin is contacted in chloroform [112]. The National Institute for Occupational Safety and Health (NIOSH) set two limits for CHCl3, recommended exposure limit of 2 ppm (for 60 min) based on risk evaluations using human or animal health effects data, and permissible exposure limit (PEL) of 50 ppm as carcinogen substance with targeted organs such liver, kidneys, and central nervous system [113]. Sharma et al. [25] fabricated chemically synthesized copper/PANI nanocomposite for $CHCl_3$ detection in the range of (10-100ppm). The sensitivity values ($\Delta R/R$) got for different $CHCl_3$ concentrations were found in the range of (1.5-3.5). However, at higher concentration, the observed ($\Delta R/R$) appears to drops amazingly, which might be because of low concentration of accessible metal clusters and bringing about the diffusion of chloroform molecules in the matrix. However at low concentration ordinarily 10ppm, ($\Delta R/R$) decreases obviously on progressive exposures to chloroform suggestive of a competent interaction of analyte at dopant sites of the host polymer. In this manner from above, unmistakably metal cluster incorporated conducting polymer can specifically and effectively be utilized as chemical sensor [25].

Methanol (HCHO) is widely used in industry and in many household products (drugs, perfumes, colors, dyes, antifreeze, etc. It is flammable, explosive, toxic and fatal to human beings even in modest concentrations. The U.S-NIOSH has recommended the short-term exposure limit of 800 ppm [114]. Athawale et al. [27] fabricated the PANI/Pd nanocomposite for methanol sensing. The experimental results revealed a very high response, to the order of ~104 magnitudes, for methanol (2000 ppm). In the case of PANI/Pd nanocomposite, Pd is acting as a catalyst for reduction of imine nitrogen in PANI by methanol. It can be also be seen that PANI/Pd nanocomposite selectively monitor methanol with an identical magnitude of response in the mixture of VOCs, but take longer response time [27]. Ma et al. [115] deposited PANI–TiO_2 nanocomposite film on interdigitated carbon paste electrodes via a spin coating and immersion method for detection of trimethylamine $N(CH_3)_3$ at RT. This PANI–TiO_2 nanocomposite film exhibited gas sensitivity to $N(CH_3)_3$, is 5.14×10^{-7} mol mL^{-1}. It took about 180 s to reach three orders of magnitude for the value of gas-sensitivity, 450 s to

reach five orders and was selective to analogous gasses [115]. The sensing film exhibited reproducibility, stability, and easy recovery with high-purity N_2 at RT.

Wang et al. [116] fabricated the sensor for VOCs gas sensing. The sensor was fabricated by using PANI intercalated MoO_3 thin films, (PANI) x MoO_3, on $LaAlO_3(100)$ (LAO) substrate. Typical response (signal (Rg/Ra)) of (PANI) x MoO_3 thin film to selected VOCs with a concentration of 50ppm with carrier N_2 gas. An increase in the response signal Rg/Ra by 8.0% within 600 s (10 min) at 30 °C was observed upon exposure to formaldehyde (HCHO) vapor and an increase in Rg/Ra by 3.8% in response to acetaldehyde (CH_3CHO) was also observed [116]. The experimental data clearly predict that (PANI)x MoO_3 exhibits distinct sensitivity to formaldehyde (HCHO) and acetaldehyde (CH_3CHO) vapors. While it was also observed that (PANI)x MoO_3 with other polar gaseous species, (such as chloroform, methanol, and ethanol) used to show very weak sensitivity. Whereas, (PANI)x MoO_3 sensor does not show any response to acetone, toluene, and xylene.

Geng et al. [117] fabricated the PANI/SnO_2 nanocomposite synthesis by a hydrothermal method for detection of ethanol (C_2H_5OH) or acetone $(CH_3)_2CO$ [117]. XRD results demonstrate that the PANI/SnO_2 nanocomposite has the same profile as pure SnO_2, showing that the crystal structure of SnO_2 is not altered by PANI. The gas detecting test for (C_2H_5OH and $(CH_3)_2CO$) was done at a fixed humidity of 60% and the operation temperatures were 30, 60 and 90°C. In the gas detecting study, it was seen that the PANI/SnO_2 nanocomposite had no gas sensitivity to ethanol or acetone when worked at 30°C. However, when worked at 60 or 90 °C, it was sensitive to low concentration of ethanol and acetone. But the most extreme reaction was seen at 90°C. The t_{res} to C_2H_5OH and $(CH_3)_2CO$ was 23–43 s and 16–20 s, individually, at 90°C, and the t_{rec} was 16–28 s and 35–48 s, separately [117]. The possible sensing mechanism was recommended to be related to the presence of p–n heterojunctions in the PANI/SnO_2 nanocomposite.

Itoh et al. [118] reported the poly(N-methylaniline)/MoO_3 ((PNMA)xMoO_3) nanocomposite is formed by an intercalation process to ion-exchange sodium ions for PNMA into MoO_3 interlayers for VOC sensor. This nanocomposite is found to be made of grains (~500 nm). (PNMA)xMoO_3 nanocomposite is found to exhibit increasing resistive responses (~1–10 ppm) aldehydic gases and these resistive responses indicate good reproducibility in its response, indicating that the can absorb and desorb aldehydic gasses within several minutes [118]. The sensitivity of the (PNMA)xMoO_3 nanocomposite, whose organic component is a

PANI derivative, to CH_3CHO is nearly similar to HCHO. Itoh et al. [119] reported layered organic–inorganic nanocomposite films of molybdenum oxide (MoO_3) with PANI, and poly(o-anisidine) (PoANIS) formed by a modified intercalation process to probe the effect of aldehyde (HCHO and CH_3CHO). However, (PANI)xMoO_3 and (PoANIS)xMoO_3 thin films exhibited enhanced response magnitude (S = 6%) as a function of resistance when exposed to HCHO and CH_3CHO in the range of (25–400 ppb) at 30°C .

Yang & Liau, reported the fabrication of nanostructured PANI films from polystyrene (PS)-PANI core-shell particles for the sensing of different dry gas flow, C_2H_5OH, HCl, and NH_3. The experimental result clearly depicts that large surface area and porosity, results in highly sensitive and fast response to different conditions, especially to dry gas flow and ethanol vapor [120]. Choudhury fabricated the PANI/Ag nanocomposite for the detection of ethanol. Choudhury experimentally reported that during ethanol exposure in the presence of AgNPs in PANI/Ag nanocomposite, the faster protonation–deprotonation of PANI takes place. The sensor response of > 2.0 and response time of 10–52 s for 2.5 mol% Ag was observed [28].

Lu et al. [121] fabricated a layer-by-layer PANI NPs–MWNT film of PANI NPs and MWCNT onto interdigitated electrodes for fabrication of stable chemiresistive sensors for methanol (CH_3OH), toluene ($C_6H_5CH_3$), and chloroform ($CHCl_3$) detection with reproducible response upon chemical cycling. Double percolated conductive networks in PANI (1%)-MWCNT (0.005%) nanocomposite resulted in both higher sensitivity (relative amplitude ~1.1%) and selectivity than other formulations, demonstrating a positive synergy [121]. Barkade et al. [23] reported the fabrication of PANI-Ag nanocomposite by an ultrasound assisted in situ mini-emulsion polymerization of ANI along with different loading of AgNPs for ethanol (C_2H_5OH) sensing. Sensing measurements were performed at different C_2H_5OH vapor concentrations (75–200 ppm). It can be observed that the nanocomposite shows a linear response (up to 100 ppm). Further, the change in resistance is found independent of concentration. The increase in resistance of sensor on exposure to C_2H_5OH may originate due to the interaction of –OH groups of ethanol molecules and nitrogen of polyaniline, leading to electron delocalization and charge transport through the polymer chain. In comparison to pure PANI, sensor response of PANI-Ag nanocomposite shows more stability as well as good reproducibility to C_2H_5OH vapors under the same condition. Steady linear response up to 2100 s was observed in PANI-Ag film sensor to C_2H_5OH (100 ppm) which on further increase in time leads to saturation of the nanocomposite film. This can be attributed to

decrease in available free volume for vapor permeability into the nanocomposite. The response time (at 100–200 ppm C_2H_5OH) of pure PANI sensor is recorded (within 21–23 min), which is decreased to (15–11), (13–10) and (8–6) min for the PANI-Ag nanocomposite sensor containing 0.5, 1.5 and 2 wt % of Ag, respectively [23].

Li et al. [122] fabricated PANI-MWCNT (mass ratio 4:1) nanocomposite for hydrocarbon detection. This PANI-MWCNT (mass ratio 4:1) nanocomposite sensor display a response of aromatic hydrocarbon vapors concentrations (200−1000 ppm) due to an increase in conductivity, and the maximum response (0.31%) was measured at 1000 ppm [122]. The increase in conductivity of PANI after gas exposure has been attributed to physical interactions due to dipole−dipole interactions that uncoil the polymer chain and decrease the hopping distance for the charge carriers.

Triethylamine $\{N(CH_2CH_3)_3\}$ is also one of the volatile organic compounds (VOCs) with a strong ammonia smell, which is flammable, and combustible. It can cause pulmonary edema and even death. The permissible exposure limit (PEL) for $N(CH_2CH_3)_3$ recommended by the US-OSHA is 25 ppm (8- hour work shift). Li et al. [123] reported the PANI/Ag nanocomposite for detection of triethylamine and toluene. The suggested mechanism for sensor response was based on chemisorption and diffusion model. Li et al. [124] fabricated the triethylamine vapor sensor. The sensor was fabricated by using MWCNTs-g-sodium polystyrene sulfonate (NaPSS) deposited on an interdigitated Au electrode decorated with a layer of positively charged poly (diallyl dimethyl ammonium chloride) by a self-assembly method. It was found that the composite exhibited a linear response to the vapor in the range of 0.5-8 ppm with the highest sensitivity of ~80%, which is much higher than that of MWNTs and PANI separately, and an obvious synergetic effect was observed. In addition, the detection limit was as low as the ppb level, and reversible and relatively fast responses (tres~200 s and ~10 min for sensing and recovery, respectively) were observed. The sensing characteristics are highly related to the gas responses of PANI, and a sensing mechanism considering the interaction of MWNTs and PANI was proposed.

2.7. PANI-based nanocomposite for LPG Detection

LPG is odorless and colorless and generates less emission than petroleum while burning. But, LPG is highly inflammable and must, therefore, be stored away from sources of ignition and thus their detection is very crucial at RT. Joshi et al. [125] reported the use of n-CdSe/p-

PANI nanocomposite for LPG sensing wherein the response was a result of the sensor's modified depletion layer. Sensor Response of ~70% for 0.08 vol% LPG was observed.

Dhawale et al. have carried out a lot of work focusing on PANI-based nanocomposite for LPG sensing at RT over the recent years. They fabricated a device with excellent stability, short response and recovery times, and shows significant selectivity towards LPG as compared to N_2 and CO_2. They too ascribed the sensor's response to a change in the barrier potential of the heterojunction.PANI/TiO_2; Response ~63% for 0.1 vol% LPG [126], n-CdS/p-PANI; Response ~80% for 1040 ppm LPG [127]. Dhawale et al. [128] also reported LPG sensor based on a p-PANI/n-TiO_2 heterojunction at RT (300K). The fabrication of heterojunction sensor was performed using electrochemically deposited polyaniline on chemically deposited TiO_2 on a stainless steel substrate. The p-PANI/n-TiO_2 sensor is known to showed the increase in response from (15 to 63%) with an increase in LPG concentration from (0.04 to 0.1 vol %). The sensor shows the maximum gas response of 63% at 0.1 vol%. At 0.12 vol% of LPG, the response decreased to 25%. It is also well revealed that the tres decreased from (200 to 140 s) when LPG concentration increased from (0.02 to 0.1 vol %). The reason for this may be due to the presence of sufficient gas molecules at the interface of the junction for reaction to occur.

Sen et al. [129] reported the detection of LPG by PANI/g-Fe_2O_3 nanocomposite at room temperature. Sensor Response of 1.3 for 200 ppm LPG was observed. Sen et al., based on the experimental investigation, proposed the plausible mechanism for the detection of LPG. The author suggested the sensing is the results of an increase in the depletion depth due to the adsorption of gas molecules at the depletion region of the p–n heterojunction [129]. Bhanvase et al. [130] reported the fabrication of LPG sensor by using PANI and PANI/$ZnMoO_4$ nanocomposite thin film with different loading of $ZnMoO_4$ (ZM) NPs. It was observed that in PANI film, the sensor response is found to increase up to 1200 ppm, however, in the case of PANI/ZM nanocomposite materials, it is found to be increased up to 1400 ppm. Sensor response for PANI and PANI/ZM nanocomposite sensor for LPG concentration (800-1800 ppm) was found to be (14.2% to 35.6%) and (20.6–45.8%) respectively. The response and recovery time characteristics of PANI/ZM nanocomposite sensor for an exposure of (1800 ppm) of LPG at RT were found to be 600 s and 840 s, respectively [130]. The graphene/PANI thin films sensor has fast response and good reproducibility for NH_3 gas.

Patil and his co-worker reported the fabrication of sensitive and selective LPG sensor based on electrospun nanofibers (NF) of PANI/ ZnO nanocomposites [131]. In the case of PANI NF, sensitivity increased from (1.11% to 7.33%) at 36°C. But with an increase in temperature (36°C to 90° C) the sensitivity decreases from (7.33% to 1.25%). While same happens in the case of PANI/ZnO NF, the sensitivity factor increased from (4.55% to 8.73% at 36°C) but as the temperature increased from (36°C to 90°C), the sensitivity decrease from (8.73% to 0.7%) [131].It was observed that with the addition of ZnO in polymer matrix results in an increase in the band gap by which, causes decrease in electrical conductivity, but causes the enhancement of sensing properties. The t_{res} was found to be 100 s for PANI/ZnO and 110 s for pure PANI. The t_{rec} was long i.e. 185 s for PANI/ZnO and 195 s for pure PANI at (1000ppm concentration) for LPG [91]. There are different methods used by different workers to form PANI nanofibers composites [132-136]. Khened et al. [137] reported Polyaniline (PANI) / Barium zirconate ($BaZrO_3$) composites for LPG sensing. The composite was prepared by in situ polymerization with 10, 20, 30, 40, 50 wt% of $BaZrO_3$ in polyaniline 1000-40000 ppm LPG, Sensitivity 1% at 40000 ppm for 50 wt% $BaZrO_3$ in PANI. Joshi et al. [138] reported *n*-CdTe/*p*-polyaniline heterojunction-based room temperature LPG sensor. The *n*-CdTe/*p*-polyaniline heterojunction sensor shows the maximum response ~67.7% for 0.14 vol% of LPG at RT (300 K). The response increased from (30% to 67.7%) with increasing the LPG concentration (0.02–0.14 vol%). At 0.16 vol%, it decreased to 50%. The reason may be due to the recombination of carriers. The t_{res} was found to be in the range of 80 and 300 s depending on the LPG concentration and the t_{rec} was about 600 s.

Sen et al. [139] reported Polyaniline/ferric oxide (PANI/-Fe_2O_3) NC films for LPG sensing at RT. The PANi/-Fe_2O_3 NC films were studied for their response to LPG at (50–200 ppm) LPG concentrations. The maximum response for PANI/-Fe_2O_3 (3 wt %) NC films for 50 ppm LPG were found to be (0.5%) with a response time of 60 s. The sensing mechanism pertains to a change in the depletion region of the p–n junction formed between PANI and -Fe_2O_3 as a result of electronic charge transfer between the gas molecules and the sensor. Shinde et al. [140] reported the fabrication of PANI/Cu_2ZnSnS_4 (CZTS) thin film based heterostructure as room temperature LPG sensor. The maximum gas response of 44% was observed at 0.06 vol% of LPG for PANI/CZTS heterojunction based sensor. The LPG response of heterojunction was decreased from (44 to 12%) at the relative humidity of 90%. PANI/CZTS heterojunction shows good stability and fast response and recovery time periods.

2.8. PANI-based nanocomposite for CO_2 Detection

Carbon dioxide (CO_2) is a colorless, odorless, noncombustible gas. It is broadly realized that CO_2 is the essential greenhouse gas discharged through human exercises. The rise in the level of the CO_2 concentration in the air since the industrial revolution has assumed a basic part in a global warming alteration and atmosphere change. The US-OSHA exposure limits of CO_2 are 10,000 ppm [8-hour Time weighted average **(**TWA**)]** and 30,000 ppm [15-minute short-term exposure limit (STEL)] are appropriate. The worry of a global warming alteration has motivated serious research on the detection, capture and storage of CO_2. Nemade and Waghuley, fabricated thick films of chemically synthesized cerium (Ce) doped PANI were prepared by screen-printing on a glass substrate for CO_2 gas sensing at RT [141]. It is directly notable from the plot that the sensing response decreases with an increase in the molar concentration of CeO_2. This shows that lower concentrations of CeO_2 result in improved sensing response. The resistance of all Ce-doped PANI films increased with an increase CO_2 gas concentration. The decrease in sensing response was observed with increasing concentration of Ce in PANI. O_2^- ions readily form weak bonds with π-electron clouds of PANI. The O_2^- ions adsorb onto the surface of the material which removes electrons from the bulk, subsequently increasing the barrier height and the resistively [141].

Nimkar et al. [142] fabricated the PANI/TiO_2 Nanocomposite Thin Film Based chemirestive sensor for detection of CO_2 gas in the atmosphere. Sensor response for PANI/TiO_2 Nanocomposite sensor for CO_2 concentration (1000 ppm) was found to be (5%) at (35°C) and it decreases from (5-1%) with increasing temperature from (35°C to 60°C).The response and recovery time characteristics of PANI/TiO_2 Nanocomposite sensor for an exposure of (1000 ppm) of CO_2 at RT was found to be 70 s and 80 s, respectively. Therefore it is concluding that PANI/TiO_2 nanocomposite is good chemiresistor sensor for CO_2 gas at RT [142].

2.9. PANI-based nanocomposite for CO Detection

Carbon monoxide (CO) is a colorless, odorless, hazardous, and poisonous gas that is produced from industrial processes and is also present in human breath [143].The permissible exposure limit (PEL) for CO recommended by US-OSHA is 35 ppm (10-hour ceiling limit), whereas the US-NIOSH suggests a limit of 50 ppm(8-hour ceiling limit) [144].Thus there is a need for sensors to detect carbon monoxide that has become an acute necessity for both environmental monitoring and human safety perspective [145]. Mishra et al. [146] reported

the rapid and selective detection of CO at ppb level using vacuum-deposited PANI-Fe:Al (80:20) nanocomposite thin films. Using these sensors, CO could be detected in the range 0.006 to 0.3 ppm at room temperature. These sensors showed the very high sensitivity of the order of 400−600, and response times of 10 s at RT. For CO sensing (7.8 to 1000 ppm), Densakulprasert et al. [147] measured the electrical conductivity of PANI-zeolite nanocomposites as a function of precursor concentration, pore size, and the ion exchange capacity of zeolite. The highest electrical conductivities and sensitivities were obtained with the 13X zeolite, followed by the Y zeolite, and the AlMCM41 zeolite.

Sen et al. [148] fabricated the PANI/Co_3O_4 nanocomposites for their sensitivity towards carbon monoxide (CO) gas at RT. The synthesis of Co_3O_4 NPs was performed by using ultrasound assisted co-precipitation method and then incorporated into the PANI matrix. The PANI/Co_3O_4 nanocomposite sensors were found to be highly selective to CO gas at RT. A significantly high response of 0.81 has been obtained for 75 ppm CO concentration with a response time of 40 s [148].

2.10. PANI-based nanocomposite for Sulfur dioxide (SO_2) Detection

Sulfur dioxide (SO_2) is a poisonous gas with the US-OSHA PEL exposure limit of 5 ppm [149]. It attacks the human respiratory system [150] and is the major reason for acid rain [151]. Thus, its monitoring is critically required. There are very few reports in the literature about sulfur dioxide sensing by individual PANI [152–157] and WO_3 [158–161] based sensing devices, but they too lack the essential parameters required for reliable SO_2 monitoring. Betty's team had systematically studied the fabrication of nanocrystalline SnO_2–PANI heterostructure sensors for sensing trace amounts of toxic gases (2 ppm SO_2 and 50 ppb NO_2) at RT (25°C). Stability studies carried out for SnO_2–PANI) heterostructure sensors and found to have a same response over 3 months [162] .

Chaudhary and Kaur, [163] reported the fabrication of PANI–WO_3 hybrid nanocomposite with honeycomb type morphology was synthesized by in situ one-pot chemical oxidative method for sensing of SO_2. The sensor response of PANI– WO_3 hybrid nanocomposite was found to be ~10.6% which is much greater as compared to pure PANI (~4%) and negligible for WO3 for 10 ppm SO_2 at RT (30°C). In order to test the authenticity of PANI–WO_3 hybrid nanocomposite sensor studied was performed at 6 different concentration of SO_2. The results show that sensor response was ~4.3%, ~10.6%, ~24%, ~36%, ~51.5% and ~69.4% for 5 ppm, 10 ppm, 25 ppm, 40 ppm, 60 ppm and 80 ppm, of

SO2 respectively at RT. Selectivity study was also performed by the authors, for which different toxic analyte vapors, such as C_2H_5OH, CH_3OH, NH_3 and H_2S (10 ppm), at RT was used for selectivity study. The sensor response was found to be ~10.6%, ~2%, ~0.5%, ~4% and ~1.5% for SO_2, C_2H_5OH, CH_3OH, NH_3 and H_2S (10 ppm), respectively at RT. The stability and reproducibility of the sensing device were studied for four consecutive weeks. It was observed that sensor response was 10.5%, 9.9%, 9.7% and 9.68% for 1, 2, 3 and 4 weeks respectively, for 10 ppm SO_2 at RT (30°C).Thus significance feature of this sensor is that it work well at RT, which reduces the cost of power and need for complex circuitry. It also shows high selectivity, stability and reproducibility at RT.

2.11. PANI-based nanocomposite for explosives, and chemical warfare agents detection

At present, as the terrible activities are of high frequency, the detection of explosives and chemical warfare agents (CWAs) attracts an increasing attention in many fields and is becoming a hot topic for research.

2.11.1. Trinitrotoluene (TNT) $C_7H_5N_3O_6$ detection

TNT ($C_7H_5N_3O_6$) occurs as yellow, needle-like crystals and is used as an explosive. OSHA PEL for 2,4,6-trinitrotoluene (TNT) was 0.5 mg/m^3 as an 8-hour TWA, with a skin notation. Gang et al. established a prominent analytical platform for electrochemical detecting of nitroaromatic explosive compounds, such as 2,4,6-trinitrotoluene (TNT) by utilizing PANI and PANI/TiO_2 nanocomposites at RT [164]. The TiO_2 nanotubes (NTs) array was assemble through electrochemical oxidation of pure titanium in a fluorine ion-containing ethylene glycol water solution followed by annealing at 450°C in air. PANI was obtained by electrochemical polymerization from an ANI and H_2SO_4 solution. TiO_2 NTs on the pure Ti sheet were coated with PANI to form a PANI/TiO_2 NTs hybrid nanocomposite. The process for fabricating the PANI/TiO_2 NTs hybrid nanocomposite is similar to that for synthesising PANI on copper. The 25% of mass content of PANi was used for synthesis of PANI/TiO_2 NTs hybrid nanocomposite. The results clearly depicts that the TiO_2 NTs sorbs more TNT (6.90 ng mg^{-1}) than the pure titanium (0.410 ng mg^{-1}). The PANI/TiO_2 NTs hybrid nanocomposite shows the highest sorption of TNT, which is 9.78 ng mg^{-1}.

2.11.2. Cyanide detection

Cyanide agents are very dangerous compounds that are called “blood agents” and used as chemical warfare agents. So, we would like detect these compounds in low concentrations for human safety. Hosseini reported synthesises of polystyrene-graft-polyaniline (PS-g-PANI), by adding solution of APS and p-toluenesufonic acid in water

[165]. PS-g-PANI was also exposed to some cyanide compounds such as hydrocyanic acid (HCN), ethanedinitrile (C_2N_2O), cyanogen chloride (CNCl), and cyanogen bromide (CNBr). A different concentration of blood agents at 50, 100, and 150 ppm and exposed them on PS-g-PANi for 2 min. The resistivity of PS-g-PANI decreases upon exposure to tested samples. It was observed that increase in the concentration of cyanide compounds causes increase in conductivity.

2.11.3. Arsine (AsH_3) detection

Arsine (AsH_3) was proposed as a possible chemical warfare weapon before World War II. AsH_3 gas is colorless, almost odorless, and 2.5 times denser than air, as required for a blanketing effect sought in chemical warfare. AsH_3 is a very toxic gas used in the semiconductor industry with a permissible exposure level (PEL) of 50 ppb. Virji, et al., reported the fabrication of Cu (II) bromide/PANI nanofiber composite sensor for AsH_3 sensing at RT [166]. It was observed that composite shows greater response compared to the other materials used. It was found that copper(II) bromide/PANI nanofiber composite sensor have proved useful in detecting toxic gases that unmodified PANI nanofibers are not able to detect AsH_3. The AsH_3 sensors shows large electrical response under low concentrations, the use of inexpensive and inert materials and a synthetic method that is easily scalable.

2.11.4. Dimethyl-methyl-phosphonate (DMMP) $CH_3PO(OCH_3)_2$ Detection

Sarin is known to be one of the strongest nerve gas agents. Sarin is widely used in chemical warfare, producing disastrous effects within seconds after inhalation. Thus knowing to Sarin's rapid action and deadliness, the fabrication of a fast, accurate gas detection technique is paramount [167]. Dimethyl-methyl-phosphonate (DMMP) is known to a typical stimulant of Sarin which is well used by many scientists in Sarin gas-related experiments.

Chang et al. [168] worked on DMMP-sensing based on composites of MWCNTs and PANI, but their sensor was reported to show a response of 1% at 332 ppm DMMP. But the study shows that PANI results in a reduction on the response time whereas any single material of SWCNTs, MWCNTs, and PANI has a limited response. Yoo et al. [169] reported the composite sensor composed of SWCNTs and PANI, to the nerve agent simulant gas, DMMP, a typical Sarin simulant. Yoo and his co-worker fabricated the SWCNT-PANI composite by dispersing the mixed solution of SWCNT and PANI on the oxidized Si substrate between Pd electrodes. During this process large amount of SWCNT networks and PANI strands are present between the two electrodes, but for simplicity, only a single PANI

strand winding around one SWCNT is shown in figure.13a by authors. SEM image of SWCNT-PANI composite was provided in the inset of figure. 13a. Figure.13b shows TEM images of SWCNT-PANI composite, while figure 13c shows the TEM images at high magnification focussing on single strand of SWCNT-PANI composite. Thus this results clearly confirm that PANI strand wrapped around the SWCNT exhibits high-quality composites with good uniformity. The authors have used the sensor for sensing DMMP gas at RT by monitoring the change in resistance of SWCNT-PANI composite film. It was observed that when electron-donating DMMP gas come in contact with SWCNT-PANI composite film sensor, DMMP molecules are adsorbed and interact with the composite film, results in stimulating electron transfer to the composite film, as shown in Figure. 13. The DMMP gas causes increase in resistance of SWCNT-PANI composite film after interaction because SWCNTs and PANI have majority carrier (hole) density which get decreased by the transferred electrons.

<<Appropriate place for the figure. 13>>

The sensor response and t_{res} were 27.1% and 5.5 s, respectively, at 10 ppm DMMP, representing a significant improvement over the pure SWCNT network sensors. The SWCNT–PANI composite sensor response was examined at various DMMP concentrations at RT. Figure. 14(a) shows the real-time sensor sensitivities at various DMMP concentrations. The response clearly increases linearly with increased DMMP concentration, as summarized in Figure. 14(b). The linear correlation between SWCNT–PANI sensor response and DMMP concentration emerges from the recurrence of DMMP adsorption are mostly proportional to its concentration. The results clearly demonstrated a very high response, rapid response time, high reproducibility, and room-temperature operability ideal DMMP sensors.

<<Appropriate place for the figure. 14>>

Yuan and Chang reported MWNTs-Polyaniline (PANI) sensor for detection of CH_3OH, $CHCl_3$, CH_2Cl_2 and simulation chemical warfare agent (DMMP as a nerve agent) [170]. Chemoresistive multi-layer sensor was fabricated by drop-coating polyaniline (PANI) solution on chemically modify MWNTs. It was observed that upon exposure to different chemical vapors, the sensing film swell reversibility and causes changes in resistance after exposure to CH_3OH (2122 ppm), $CHCl_3$ (2238ppm), CH_2Cl_2 (481ppm) DMMP (332 ppm). MWNTs/PANI sensing films resistivity toward DMMP, CH_2Cl_2, CH_3OH and $CHCl_3$ are ~2.1

to ~22.02 % of magnitude, respectively. The sensitivity of the MWNTs/PANI sensing films drastically increased by 8 ~ 22% of exposure to DMMP and CH_2Cl_2 vapors, and 0.4 ~ 0.9% of exposure to $CHCl_3$ and CH_3OH within 300s. While when the sensing film is transfer back to dry air, the electrical resistance returned to the original value rapidly, demonstrating a good restoring performance. The MWNTs-Polyaniline (PANI) sensor also shows better resistance reproducibility and stability after four cycles of exposure to solvent vapors and a dry air.

2.11.5. Phosgene ($COCl_2$) Detection

Phosgene ($COCl_2$) is a colorless, highly toxic industrial chemical that has a low permissible exposure limit (PEL) of 0.1 ppm and an immediate danger to health and life (IDLH) limit of 2 ppm [171]. Presently it is used in the factory to make dyestuffs, polyurethane resins, plastics and pesticides and was used as a chemical weapon during World War I. During Inhalation, $COCl_2$ reacts with water in the lungs to form HCl and CO, which causes pulmonary edema, bronchial pneumonia and lung abscesses. Virji et al. [172] reported the fabrication of amine–PANI nanofiber composite materials in aqueous solution by addition of the amine solution to an aqueous suspension of PANI nanofibers. The different amines and amine salts used are ethylenediamine, ethylenediamine dihydrochloride, phenylenediamine, phenylenediamine dihydrochloride, and metanilic acid used in the synthesis of amine–polyaniline nanofiber composite materials. Virji et al. drew a conclusion that composites of PANI nanofibers with amines respond well to phosgene at concentrations 0.1 and 2ppm at 22°C and 50% RH. Amines are known to react with $COCl_2$ in a nucleophilic substitution reaction to form carbamoyl chlorides (R_2NCOCl) which can be readily dehydrohalogenated to form isocyanates (R–N=C=O) [173]. In this reaction, HCl is formed, which can dope the PANI converting it from the emeraldine base oxidation state to the emeraldine salt oxidation state. This results in two orders of magnitude increase in conductivity.

3. Conclusions

PANI-based sensors, which convert a chemical interaction into an electrical signal, covering a wide range of applications, have effectively been exhibited as proficient sensors for monitoring organic and inorganic compounds. In this review, author have explored current progress in the invention of PANI hybrid nanocomposite for gas/vapor sensors for environmental monitoring at RT. Author have also reviewed the basic principles, sensor parameter and properties of PANI-based nanocomposites and their use in various gas/vapor

sensor applications. Nanostructured PANI exhibit excellent sensing behavior because of their desired functionality and conductivity. The cited articles mention in the present review article display the structural versatility of these PANI-based nanocomposite as sensitive chemical sensors, with additional advantages of a high selectivity, a fast response and recovery time and great stability.

4. Challenges and Future Prospects

The response and recovery times and the sensitivity have encountered magnificent enhancement with impressive progress in nanotechnology over the past decades. As we know that selectivity is still a major challenge. Detecting target species in a complex environment remains a troublesome assignment, and is impeding the extensive application of conducting polymer-based sensors. Cross sensitivity means sensor exhibit homogeneous responses to the distinctive types of gases, and this character may result in false detecting. It was also observed that nanostructured based sensor have indicated poor sensitivity and moderate response time because of the functional properties which are not yet fully comprehended [12]. Does improved comprehension of functional properties will gives the chances to synthesize new nanostructured conducting polymers that will address these issues [174].

It is outstanding that there are different parameters, for example, shape and size of inorganic nanostructures, porosity, inter-phase interaction, surface and interfacial energy, catalysts activity, chemical reactivity control the response of the gas sensors. These parameters rely on the type and concentration of inorganic additives. Apart from this the ratio of the organic and inorganic materials is very crucial and need attentive optimization to accomplish great detecting of a gas sensor.

One of critical difficulties we stood up to with is the nonrepeatability of device fabrication. Hypothesis can demonstrate a heading for practice. However, till now, the mechanism of gas/vapor detecting in view of nanomaterials is not clear, and quantitative estimation is practically difficult. A great deal of consideration is yet excessively paid on the choice of nano-detecting materials to enhance the 3S concept i.e., selectivity, sensitivity and stability for the improvement of gas sensing devices. Another technique towards free-standing PANI nanofibers by enhancing the mechanical properties is another approach to upgrade the usability of PANI nanofibers for gas sensing application. In literature, we have found no or very limited sensing was performed on heavy explosive molecules like, trinitrotoluene (TNT), Dinitrotoluene (DNT), pentaerythritol tetranitrate (PETN), hexahydro-

1,3,5- triazine (RDX) etc. and chemical warfare agents like phosgene, chlorine, DMMP, arsine etc. Thus in the near future more research and investigation related to the sensing of explosives and chemical warfare agents need to be focussed. The future of PANI-based nanocomposite gas/vapor sensors looks bright. Continued progress in this field will overcome the current challenges, get through the close siege, and lead to a class of gas sensors with low power consumption, low cost, superior sensitivity, excellent selectivity, miniaturization, and long term stability for a wide range of applications in different ways such as industrial emission control, control of nuclear power plants, household security, vehicle emission control and environmental monitoring.

Acknowledgements

The author likes to express our gratitude to the National Research foundation (NRF) for financial support (Grant No: 91399). The author also acknowledge University of Johannesburg (UJ), (South Africa) for UJ Database and laboratory facility.

Conflicts of interest

The authors declare no competing financial interests.

References

[1] A. Ponzoni, E. Comini, I. Concina, M. Ferroni, M. Falasconi, E. Gobbi, V. Sberveglieri, G. Sberveglieri, Nanostructured Metal Oxide Gas Sensors, a Survey of Applications Carried out at SENSOR Lab, Brescia (Italy) in the Security and Food Quality Fields, Sensors (Basel). 12 (2012) 17023–17045.

[2] S. Pandey, G.K. Goswami, K.K. Nanda, Nanocomposite based flexible ultrasensitive resistive gas sensor for chemical reactions studies, Scientific Reports 3 (2013) 2082.

[3] S. Pandey, G.K. Goswami, K.K. Green synthesis of polysaccharide/gold nanoparticle nanocomposite: An efficient ammonia sensor, Carbohydr. Polym. 94 (2013) 229-234.

[4] S. Pandey, J. Ramontja, Rapid, facile microwave-assisted synthesis of xanthan gum grafted polyaniline for chemical sensor, International Journal of Biological Macromolecules. 89 (2016) 89-98.

[5] S. Pandey, J. Ramontja, Turning to Nanotechnology for Water Pollution Control: Applications of Nanocomposites, Focus on Sciences 2 (2) (2016) 1-10.

[6] S. Pandey, K.K. Nanda, Au Nanocomposite Based Chemiresistive Ammonia Sensor for Health Monitoring, ACS Sensors 1 (2016) 55-62.

[7] S. Pandey, K.K. Nanda, One-dimensional Nanostructure Based Chemiresistive Sensor, Nantotechnology, Vol.10: Nanosensing 2013: 10:1-16. ISBN: 1-62699-010-7, Studium Press LLC, USA .

[8] H. Shokry Hassan, A.B. Kashyout, I. Morsi, A.A.A. Nasser, H. Abuklill, Development of polypyrrole coated copper nanowires for gas sensor application, Sensing and Bio-Sensing Research 5 (2015) 50–54.

[9] A.G. MacDiarmid, Synthetic Metals: A Novel Role for Organic Polymers (Nobel Lecture). Angew. Chem., Int. Ed. 40 (2001) 2581−2590.

[10] T. Liu, C. Burger, B. Chu, Nanofabrication in Polymer Matrices. Prog. Polym. Sci. 28 (2003) 5−26.

[11] B. Adhikari, S. Majumdar, Polymers in Sensor Applications. Prog. Polym. Sci. 29 (2004) 699−766.

[12] J. Janata, M. Josowicz,, Conducting Polymers in Electronic Chemical Sensors. Nat. Mater. 2 (2003) 19−24.

[13] S. Capone, P. Siciliano, F. Quaranta, R. Rella, M. Epifani, L. Vasanelli, Analysis of vapours and foods by means of an electronic nose based on a sol−gel metal oxide sensors Array, Sens. Actuators, B 69 (2000) 230−235.

[14] W. Tsujita, A. Yoshino, H. Ishida, T. Moriizumi, Gas sensor network for air-pollution monitoring. Sens. Actuators B 110 (2005) 304−311.

[15] N. Barsan, D. Koziej, U. Weimar, Metal oxide-based gas sensor research: How to? Sens. Actuators, B 121 (2007) 18−35.

[16] P. Kunzo, P. Lobotka, M. Micusik, E. Kovacova, Palladium-free hydrogen sensor based on oxygen-plasma-treated polyaniline thin film, Sensors Actuators B Chem. 171-172 (2012) 838–845.

[17] J.B. Yadav, S.V. Jadhav, R.K. Puri, V. Puri, Properties of Vacuum Evaporated Vapour Chopped Polyaniline Thin Film: Effect of Synthesis Method, J. Phys. Conf. Ser. 114 (2008) 012037.

[18] K. Mylvaganam, L.C. Zhang, Fabrication and application of polymer composites comprising carbon nanotubes, Recent Patents Nanotechnol. 1 (2007) 59–65.

[19] H. Bai, G. Shi, Gas Sensors Based on Conducting Polymers, Sensors 7 (2007) 267–307.

[20] E.M. Genies, A. Boyle, M. Lapkowski, C. Tsintavis, Polyaniline: a historical survey, Synth. Met. 36 (1990) 139–182.

[21] Y.S. Negi, P.V. Adhyapak, Development in Polyaniline Conducting Polymers, J. Macromol. Sci.-Polym. Rev. C 42 (2002) 35–53.

[22] S. Jiang, J. Chen, J. Tang, E. Jin, L. Kong, W. Zhang, C. Wang, Au nanoparticles functionalized two-dimensional patterned conducting PANI nanobowl monolayer for gas sensor, Sensors Actuators B Chem. 140 (2009) 520–524.

[23] S.S. Barkade, J.B. Naik, S.H. Sonawane, Ultrasound assisted miniemulsion synthesis of polyaniline/Ag nanocomposite and its application for ethanol vapor sensing, Colloids Surfaces A Physicochem. Eng. Asp. 378 (2011) 94–98.

[24] P. Kunzo, P. Lobotka, E. Kováčová, Modification of polyaniline-based gas sensor by electrophoretic deposition of metal nanoparticles in ionic liquids, Key Engineering Materials 654 (2015) 224-229.

[25] S. Sharma, C. Nirkhe, S. Pethkar, A.A. Athawale, Chloroform vapour sensor based on copper/polyaniline nanocomposite, Sensors Actuators B Chem. 85 (2002)131–136.

[26] C.T.P. da Silva , V.L. Kupfer , G.R. da Silva, M.P. Moisés, M.A.G. Trindade , N.L.C. Domingues , A.W. Rinaldi, One-step electrochemical synthesis of polyaniline/metallic oxide nanoparticle (γ-Fe_2O_3) thin film, Int. J. Electrochem. Sci., 11 (2016) 5380 – 5394.

[27] A.A. Athawale, S.V. Bhagwat, P.P. Katre, Nanocomposite of Pd–polyaniline as a selective methanol sensor, Sensors Actuators B Chem. 114 (2006) 263–267.

[28] A. Choudhury, Polyaniline/silver nanocomposites: Dielectric properties and ethanol vapour sensitivity, Sensors Actuators B Chem. 138 (2009) 318–325.

[29] M.J. Fedoruk, R. Bronstein, B.D. Kerger, Ammonia exposure and hazard assessment for selected household cleaning product uses, J. Exposure Anal. Environ. Epidomiol. 15 (2005) 534–544

[30] Y. Hou, A.H. Jayatissa, Enhancement of gas sensor response of nanocrystalline zinc oxide for ammonia by plasma treatment, Appl. Surf. Sci. 309 (2014) 46–53.

[31] X. Liang, Z. Chen, H. Wu, L. Guo, C. He, B. Wang, Y. Wu, Enhanced NH_3-sensing behavior of 2, 9, 16, 23-tetrakis (2, 2, 3, 3-tetrafluoropropoxy) metal (II) phthalocyanine/multi-walled carbon nanotube hybrids: an investigation of the effects of central metals, Carbon 80 (2014) 268–278.

[32] Kumar V, Patil V, Apte A, Harale N, Patil P, Kulkarni S. Ultrasensitive Gold Nanostar-Polyaniline Composite for Ammonia Gas Sensing, Langmuir, 2015, 31 (48), 13247–13256

[33] H. Tai, Y. Jiang, G. Xu, J. Yu, X. Chen, Fabrication and gas sensitivity of polyaniline–titanium dioxide nanocomposite thin film. Sens. Actuators B 125 (2007) 644–650.

[34] Q. Chang, K. Zhao, X. Chen, M. Li, J. Liu, Preparation of Gold/Polyaniline/Multiwall Carbon Nanotube Nanocomposites and Application in Ammonia Gas Detection, J. Mater. Sci. 43 (2008) 5861−5866.

[35] K. Crowley, A. Morrin, A. Hernandez, E. O'Malley, P.G. Whitten, G.G. Wallace, M.R. Smyth, A.J. Killard, Fabrication of an ammonia gas sensor using inkjetprinted polyaniline nanoparticles, Talanta 77 (2008) 710–717.

[36] N.G. Deshpande, Y.G. Gudage, R. Sharma, J.C. Vyas, J.B. Kim, Y.P. Lee, Studies on tin oxide-intercalated polyaniline nanocomposite for ammonia gas sensing applications, Sensors and Actuators B 138 (2009) 76–84.

[37] T. Zhang, S. Mubeen, B. Yoo, N.V. Myung, M.A. Deshusses, A gas nanosensor unaffected by humidity, Nanotechnology, 20 (2009) 255501.

[38] H. Tai, Y. Jiang, G. Xie, J. Yu, Preparation, characterization and comparative NH_3-sensing characteristic studies of PANI/Inorganic oxides nanocomposite thin films, J. Mater. Sci. Technol. 26 (2010) 605−613.

[39] J.-H. Lim, N. Phiboolsirichit, S. Mubeen, M.A. Deshusses, A. Mulchandani, N.V. Myung, Electrical and gas sensing properties of polyaniline functionalized single-walled carbon nanotubes, Nanotechnology 21 (2010) 075502.

[40] J. Gong, Y. Li, Z. Hu, Z. Zhou, Y. Deng, Ultrasensitive NH_3 Gas sensor from polyaniline nanograin enchased TiO_2 fibers. J. Phys. Chem. C 114 (2010) 9970–9974.

[41] S.G. Pawar, S.L. Patil, M.A. Chougule, P.R. Godse, D.K. Bandgar, V.B. Patil, Fabrication of polyaniline/ TiO_2 nanocomposite ammonia vapor sensor, J. NanoElectron. Phys. 3 (2011) 1056–1063.

[42] J. Wojkiewicz, V. Bliznyuk, S. Carquigny, N. Elkamchi, N. Redon, T. Lasri, A. Pud, S. Reynaud, Nanostructured polyaniline-based composites for ppb range ammonia sensing, Sensors and Actuators B: Chemical 160 (2011) 1394–1403.

[43] S.L. Patil, M.A. Chougule, S.G. Pawar, S. Sen, A.V. Moholkar, J.H. Kim, V.B. Patil, Fabrication of polyaniline-ZnO nanocomposite gas sensor, Sensors & Transducers Journal, 134 (2011) 120-131

[44] I. Venditti, I. Fratoddi, M.V. Russo, A. Bearzotti, A nanostructured composite based on polyaniline and gold nanoparticles: synthesis and gas sensing properties, Nanotechnology 24, 155503 (2013) 1-7.

[45] P. Kunzo, P. Lobotka, E. Kovacova, K. Chrissopoulou, L. Papoutsakis, S.H. Anastasiadis, Z. Krizanova, I. Vavra, Nanocomposites of polyaniline and titania nanoparticles for gas sensors. physica status solidi (a), 210 (2013) 2341–2347.

[46] Z. Wu, X. Chen, S. Zhu, Z. Zhou, Y. Yao, W. Quan, B. Liu, Enhanced sensitivity of ammonia sensor using graphene/polyaniline nanocomposite, Sensors and Actuators B 178 (2013) 485–493.

[47] H.-D. Zhang, C.-C. Tang, Y.-Z. Long, J.-C. Zhang, R. Huanga, J.-J. Li, C.-Z. Gu, High-sensitivity gas sensors based on arranged polyaniline/PMMA composite fibers, Sens.Actuators, A, 219 (2014) 123–127.

[48] S. Abdulla, L.T. Mathew, B. Pullithadathil, Highly sensitive, room temperature gas sensor based on polyaniline-multiwalled carbon nanotubes (PANI/MWCNTs) nanocomposite for trace-level ammonia detection, Sensors and Actuators B 221 (2015) 1523–1534.

[49] Z. Pang, Z. Yang, Y. Chen, J. Zhang, Q. Wang, F. Huang, Q. Wei, A room temperature ammonia gas sensor based on cellulose/TiO_2/PANI composite nanofibers, Colloids and Surfaces A: Physicochem. Eng. Aspects 494 (2016) 248–255.

[50] Y. Guo, T. Wang, F. Chen, X. Sun, X. Li, Z. Yu, P. Wan, X. Chen, Hierarchical graphene–polyaniline nanocomposite films for high-performance flexible electronic gas sensors, Nanoscale, 8 (2016) 12073-12080

[51] L Zhihu, Z. Xucheng, S. Jiyong, Z. Xiaobo, H. Xiaowei, H. E. Tahir, M. Holmes, Fast response ammonia sensor based on porous thin film of polyaniline/sulfonated nickel phthalocyanine composites, Sensors and Actuators B 226 (2016) 553–562

[52] G.D. Khuspe, D.K. Bandgar, S. Sen, V.B. Patil, Fussy nanofibrous network of polyaniline (PANI) for NH_3 detection, Synth. Met. 162 (2012) 1822–1827.

[53] S. Chen, G. Sun, High sensitivity ammonia sensor using a hierarchical polyaniline/poly(ethylene-co-glycidyl methacrylate) nanofibrous composite membrane, ACS Appl. Mater. Interf. 5 (2013) 6473–6477.

[54] G.D. Khuspe, S.T. Navale, M.A. Chougule, V.B. Patil, Ammonia gas sensing properties of CSA doped PANi-SnO_2 nanohybrid thin films, Synth. Met. 185–186 (2013) 1–8.

[55] H. Tai, X. Xu, Z. Ye, C. Liu, G. Xie, Y. Jiang, P–P heterojunction sensor of selfassembled polyaniline nano-thin film/microstructure silicon array for NH_3 detection, Chem. Phys. Lett. 621 (2015) 58–64.

[56] K.-P. Yoo, K.-H. Kwon, N.-K. Min, M.J. Lee, C.J. Lee, Effects of O_2 plasma treatment on NH_3 sensing characteristics of multiwall carbon nanotube/polyaniline composite films, Sens. Actuators B: Chem. 143 (2009) 333–340.

[57] X. Huang, N. Hu, L. Zhang, L. Wei, H. Wei, Y. Zhang, The NH_3 sensing properties of gas sensors based on aniline reduced graphene oxide, Synthetic Metals 185–186 (2013) 25– 30.

[58] J. N. Gavgani,, A. Hasani,, M. Nourib, ,M. Mahyari,, A. Salehi,, Highly sensitive and flexible ammonia sensor based on S and N co-doped graphene quantum dots/polyaniline hybrid at room temperature , Sensors and Actuators B 229 (2016) 239–248.

[59] J. Wang, B. Singh, J.H. Park, S. Rathi, I. Lee, S. Maeng, H. Joh, C. Lee, G. Kim, Dielectrophoresis of graphene oxide nanostructures for hydrogen gas sensor at room temperature, Sens. Actuators B: Chem. 194 (4) (2014) 296–302.

[60] Z. Wang, Z. Li, T. Jiang, X. Xu, C. Wang, Ultrasensitive hydrogen sensor based on Pd^0-loaded SnO_2 electrospun nanofibers at room temperature, Appl. Mater. Interfaces 5 (6) (2013) 2013–2021.

[61] M. Ramanathan, G. Skudlarek, H. Wang, S.B. Darling, Crossover behavior in the hydrogen sensing mechanism for palladium ultrathin films, Nanotechnology 21 (12) (2010) 125501–125506 (6).

[62] A.Z. Sadek, W. Wlodarski, K. Shin, R.B. Kaner, K. Kalantarzadeh, A Polyaniline/WO_3 Nanofiber Composite Based ZnO/64°YX $LiNbO_3$ SAW Hydrogen Gas Sensor. Synth. Met. 158 (2008) 29–32.

[63] L. Al-Mashat, K. Shin, K. Kalantar-zadeh, J.D. Plessis, S.H. Han, R.W. Kojima, R.B. Kaner, D. Li, X. Gou, S.J. Ippolito, W. Wlodarski, Graphene/Polyaniline Nanocomposite for Hydrogen Sensing, J. Phys. Chem. C, 114 (2010)16168–16173.

[64] S. Nasirian, H.M. Moghaddam, Hydrogen gas sensing based on polyaniline/anatase titania nanocomposite, International Journal of Hydrogen Energy Volume 39 (2014) 630–642.

[65] H.J. Sharma, D.V. Jamkar, S.B. Kondawar, Electrospun nanofibers of conducting polyaniline/Al-SnO_2 composites for hydrogen sensing applications. Procedia Materials Science 10 (2015) 186 – 194.

[66] S. Srivastava, S.S. Sharma, S. Agrawal, S. Kumar, M. Singh, Y.K. Vijay, Study of chemiresistor type CNT doped polyaniline gas sensor, Synthetic Metals 160 (2010) 529–534

[67] S. Srivastava, S. Kumar, Y.K. Vijay, Preparation and characterization of tantalum/polyaniline composite based chemiresistor type sensor for hydrogen gas sensing application, International Journal of Hydrogen Energy 3 7 (2 0 1 2) 3 8 2 5 -3 8 3 2

[68] A.Z. Sadek, C.O. Baker, D.A. Powell, W. Wlodarski, R.B. Kaner, K. Kalantarzadeh, Polyaniline nanofiber based surface acoustic wave gas sensors–effect of nanofiber diameter on H_2 response, IEEE Sensors J. 7 (2007) 213–217

[69] S.J. Huang, S. Virji, B.H. Weiller, R.B. Kaner. Polyaniline nanofibers: facile synthesis and chemical sensors, J Am Chem Soc 125 (2003) 314-315.

[70] S Nasirian, H. M. Moghaddam, Polyaniline assisted by TiO_2:SnO_2nanoparticles as a hydrogen gas sensor at environmental conditions, Applied Surface Science 328 (2015) 395–404

[71] Richard, G., & Griskey, Polymer process engineering. USA: International Thomson publishing (1995).

[72] S Pandey, GK Goswami, KK Nanda, Green Synthesis of Biopolymer-Silver nanoparticle Nanocomposite: An optical Sensor for Ammonia Detection. International Journal Of biological Macromolecules. 51 (2012) 583-589.

[73] V Singh, S Tiwari, S Pandey, Preeti, R Sanghi, *Cassia Grandis* Seed Gum-*graft*-poly(acrylamide)-silica Hybrid: An Excellent Cadmium (II) Adsorbent, Adv. Material Letters 6 (2015)19-26.

[74] S Pandey, J Ramontja, Sodium alginate stabilized silver nanoparticles–silica nanohybrid and their antibacterial Characteristics, International Journal Of biological Macromolecules. 93A (2016) 712-723. http://dx.doi.org/10.1016/j.ijbiomac.2016.09.033

[75] S Pandey, J Ramontja, Natural Bentonite Clay and Its Composites for Dye Removal: Current State and Future Potential. American Journal of Chemistry and Applications 3 (2) (2016) 8-19.

[76] S Pandey, Facile approach to synthesize chitosan based composite—Characterization and cadmium (II) ion adsorption studies. Carbohydrate Polymers 134 (2015) 646–656.

[77] S Pandey, S B Mishra, Catalytic reduction of p-nitrophenol by using platinum nanoparticles stabilised by guar gum, Carbohydrate Polymer 113 (2014) 525-531.

[78] S Pandey, S B Mishra, Chromatographic resolution of racemic α-amino acids: Chiral stationary phase derived from modified xanthan gum. Carbohydrate Polymer. 92 (2013) 2201– 2205.

1333 [79] S Pandey, S B Mishra, Microwave synthesized xanthan gum-g-poly(ethylacrylate):
1334 An efficient Pb^{2+} ion binder, Carbohydrate Polymer. 90 (2012) 370-379.

1335 [80] S Pandey, SB. Mishra, Graft copolymerization of ethyl acrylate onto xanthan gum,
1336 using potassium peroxydisulphate as an initiator, International Journal of
1337 Biological macromolecules. 49 (2011) 527–535.

1338 [81] S Pandey, SB Mishra, Organic-inorganic hybrid of Chitosan / Organoclay
1339 bionanocomposites for Hexavalent Chromium uptake, Journal of colloid and
1340 interface science. 361 (2011) 509–520.

1341 [82] S Pandey, SB. Mishra, Sol–gel derived organic–inorganic hybrid materials:
1342 synthesis, characterizations and applications, Journal of Sol-gel Science and
1343 Technology, 59 (2011) 73-94.

1344 [83] V Singh , S K Singh, S Pandey, R Sanghi, Synthesis and characterization of guar
1345 gum templated hybrid nano silica. International Journal of biological
1346 macromolecules. 49 (2011) 233– 240.

1347 [84] V Singh, S K Singh, S Pandey, P Kumar, Sol–gel synthesis and characterization of
1348 adsorbent and photoluminescent nanocomposites of starch and silica, Journal of
1349 Non-Crystalline Solids. 357 (2011) 194–201.

1350 [85] V Singh, S K Singh, S Pandey, R Sanghi. Adsorption behavior of potato starch-
1351 silica nanobiocomposite. Adv. Material Letters 1(2010) 40-47.

1352 [86] V. Singh, PL Kumari, A Tiwari, S Pandey, Alumina supported microwave synthesis
1353 of Cassia marginata seed gum-graft-poly(acrylamide), Journal of applied and
1354 polymer science. 117(2010) 3630-3638.

1355 [87] V Singh, S Pandey, S K Singh, R Sanghi, Removal of cadmium from aqueous
1356 solutions by adsorption poly(acrylamide) modified guar gum-silica
1357 nanocomposites. Separation and purification technology 67 (2009) 251-261.

1358 [88] V Singh, P Kumari, S Pandey, T Narayan, Removal of Chromium (VI) using poly
1359 (methylacrylate) functionalized guar gum . Bio resource Technology 100
1360 (2009)1977-1982.

1361 [89] V Singh, S Pandey, S K Singh, R Sanghi, Sol-gel polycondensation of
1362 tetraethoxysilane in ethanol in presence of vinyl modified guar gum: synthesis of
1363 novel adsorbent materials. Journal Sol-gel Science and Technology 47 (2008),
1364 58-67.

1365 [90] V Singh, S Pandey, S K Singh, R Sanghi, Synthesis of Novel Nanocomposites of
1366 Silica and Guar Gum: Efficient Zinc Ion Binder. Journal of Fudan University
1367 (Natural Science), 46, (5) (2007) 155.

1368 [91] V Singh, A Tiwari, S Pandey, S K Singh, R Sanghi, Synthesis and characterization
1369 of novel saponified guar graft-polyacrylonitrile/silica nanocomposite materials,
1370 Journal of Applied polymer science 104, (2007), 536-544.

1371 [92] V Singh, A. Tiwari, S Pandey, S K Singh, Peroxydisulfate initiated synthesis of
1372 potato starch-graft- poly(acrylonitrile) under microwave irradiation, xPress
1373 polymer letters 1(2007) 51-58.

[93] V Singh, A Tiwari, S Pandey S K Singh, Microwave accelerated synthesis and characterization of potato starch-g-poly (acrylamide), Starch/Starke, 58 (2006) 536-543.

[94] Wei Li, D. M. Jang, S. Y. An, D. Kim, S-K. Hong, H. Kim, Polyaniline–chitosan nanocomposite: High performance hydrogen sensor from new principle, Sensors and Actuators B 160 (2011) 1020– 1025.

[95] Hydrogen chloride/hydrochloric acid Toxicological overview (2007) version 1, www.hpa.org.uk/webc/HPAwebFile/HPAweb C/1194947386706

[96] TOXNET, National Library of Medicine, National Institutes of Health, www.toxnet.nlm.nih.gov

[97] Assessment of Exposure-Response Functions for Rocket-Emission Toxicants. Subcommittee on Rocket-Emission Toxicants, National Research Council, ISBN: 0-309-59213-5, 228 pages, 6 x 9, National academy press Washington, D.C. (1998). https://www.ncbi.nlm.nih.gov/books/NBK230426/

[98] S.C.K. Mishra, P. Mathur, M. Yadav, M.K. Tiwari, S.C. Garg, P. Tripathi, Preparation and characterization of vacuum deposited semiconducting nanocrystalline polymeric thin film sensors for detection of HCl. Polymer 45 (2004) 8623–8628.

[99] J Yun, S Jeon, H-Il Kim' Improvement of NO Gas Sensing Properties of Polyaniline/MWCNT Composite by Photocatalytic Effect of TiO_2, J. Nanomater., 2013, (2013) 184345.

[100] H. Xu, X. Chen, J. Zhang, J. Wang, B. Cao, D. Cui, $CuNO_2$ gas sensing with SnO_2–ZnO/PANI composite thick film fabricated from porous nanosolid, Sens. Actuators, B 176 (2013) 166–173.

[101] A. Kaushik, R. Khan, V. Gupta, B.D. Malhotra, S. Ahmad, S.P. Singh, Hybrid cross-linked polyaniline-WO_3 nanocomposite thin film for NOx gas sensing. J. Nanosci. Nanotechnol. 9 (2009) 1792–1796.

[102] S. Prakash, S. Rajesh, S.R. Singh, C. Karunakaran, V. Vasu, Electrochemical Incorporation of hemin in a ZnO–PPy nanocomposite on a Pt electrode as NOx sensor. Analyst 137 (2012)5874.

[103] A. Sharma, M. Tomar, V. Gupta, A. Badola, N. Goswami, Polyaniline/SnO_2 Nanocomposite Sensor for NO_2 Gas Sensing at low operating temperature, International Journal of Nanoscience, 14 (2015) 4.

[104] H. Xu, D. Ju, W. Li, H. Gong, J. Zhang, J. Wang, B. Cao, Low-working-temperature, fast-response-speed NO2 sensor withnanoporous-SnO2/polyaniline double-layered film, Sensors and Actuators B 224 (2016) 654–660.

[105] M.D. Shirsat, M.A. Bangar, M.A. Deshusses, N.V. Myung, A. Mulchandani, Polyaniline nanowires-gold nanoparticles hybrid network based chemiresistive hydrogen sulfide sensor, Appl. Phys. Lett. 94 (2009) 083502–083504.

[106] K. Crowley, A. Morrin, R.L. Shepherd, M-in-h. Panhuis, G.G. Wallace, M.R. Smyth, A.J. Killard, Fabrication of polyaniline-based gas sensors using piezoelectric inkjet and screen printing for the detection of hydrogen sulfide, IEEE Sens. J. 10 (2010) 1419–1426.

[107] B.T. Raut, M.A. Chougule, S.R. Nalage, D.S. Dalavi, S. Mali, P.S. Patil, V.B. Patil, CSA doped polyaniline/CdS organic– Inorganic nanohybrid: Physical and Gas Sensing Properties. Ceram. Int. 38 (2012) 5501–5506.

[108] B.T. Raut, P.R. Godse, S.G. Pawar, M.A. Chougule, D.K. Bandgar, V.B. Patil, Novel method for fabrication of polyaniline–CdS sensor for H_2S gas detection, Measurement 45 (2012) 94–100.

[109] A. Mekki, N. Joshi, A. Singh, Z. Salmi, P. Jha, P. Decorse, H_2S sensing using in situ-polymerized polyaniline–silver nanocomposite films on flexible substrates, Org. Electron. 15 (2014) 71–81.

[110] J.M. Slater, E.J. Watt, N.J. Freeman, I.P. May, D.J. Weir, Gas and vapor detection with poly (pyrrole) gas sensors, Analyst 117 (1992) 1265–1270.

[111] G. Aggazzotti, G. Fantuzzi, E. Righi, G. Predieri, Blood and breath analyses as biological indicators of exposure to trihalomethanes in indoor swimming pools, Sci. Total Environ. 217 (1998) 155–163

[112] P. Perillo, D. Rodríguez. A room temperature chloroform sensor using TiO_2 nanotubes, Sens Actuators B 193 (2014) 263–266.

[113] S. Liu, Y. Yao, S. Lu, K. Aldous, X. Ding, C. Mei, J. Gu. The role of renal proximal tubule P450 enzymes in chloroform-induced nephrotoxicity: Utility of renal specific P450 reductase knockout mouse models. Toxicol Appl Pharmacol 272 (2013) 230–237

[114] Robust Summary of Toxicity of Methanol", U.S. EPA, March 23, 2001.

[115] X. Ma, M. Wang, G. Li, H. Chen, R. Bai, Preparation of Polyaniline–TiO_2 Composite Film with in Situ Polymerization Approach and its Gas-Sensitivity at Room Temperature. Mater. Chem. Phys. 98 (2006) 241–247.

[116] J. Wang, I. Matsubara, N. Murayama, S. Woosuck, N. Izu, The preparation of polyaniline intercalated MoO_3 thin film and its sensitivity to volatile organic compounds. Thin Solid Films 514 (2006) 329–333.

[117] L. Geng, Y. Zhao, X. Huang, S. Wang, S. Zhang, S. Wu, Characterization and gas sensitivity study of polyaniline/SnO_2 hybrid material prepared by hydro-thermal route, Sens. Actuators B 120 (2007) 568–572.

[118] T. Itoh, I. Matsubara, W. Shin, N. Izu, Synthesis and characterization of layered organic/Inorganic hybrid thin films based on molybdenum trioxide with poly(N-methylaniline) for VOC sensor. Mater. Lett. 61 (2007) 4031–4034.

[119] T. Itoh, I. Matsubara, W. Shin, N. Izu, M. Nishibori, Preparation of layered organic–Inorganic nanohybrid thin films of molybdenum trioxide with polyaniline derivatives for aldehyde gases sensors of several tens ppb level, Sens. Actuators, B 128 (2008) 512–520.

[120] L.Y. Yang, W.B. Liau, Environmental responses of nanostructured polyaniline films based on polystyrene–polyaniline core–shell particles, Mater. Chem.Phys. 115 (2009) 28–32.

[121] J. Lu, B.J. Park, B. Kumar, M. Castro, H.J. Choi, J.-F. Feller, Polyaniline nanoparticle–carbon nanotube hybrid network vapour sensors with switchable chemo-electrical polarity. Nanotechnology 21 (2010) 255501.

[122] W. Li, D. Kim, Polyaniline/Multiwall carbon nanotube nanocomposite for detecting aromatic hydrocarbon vapors. J. Mater. Sci. 46 (2011) 1857–1861.

[123] Z.-F. Li, F.D. Blum, M.F. Bertino, C.-S. Kim, Understanding the response of nanostructured polyaniline gas sensors, Sens. Actuators, B 183 (2013) 419–427.

[124] Y. Li, H. Wang, X. Cao, M. Yuan, M. Yang. A composite of polyelectrolyte-grafted multi-walled carbon nanotubes and in situ polymerized polyaniline for the detection of low concentration triethylamine vapor. Nanotechnology (2008) 19 015503.

[125] S.S. Joshi, C.D. Lokhande, S.H. Han, A room temperature liquefied petroleum gas sensor based on all electrodeposited n-CdSe/p-polyaniline junction, Sens. Actuators, B 123 (2007) 240–245.

[126] D.S. Dhawale, R.R. Salunkhe, U.M. Patil, K.V. Gurav, A.M. More, C.D. Lokhande, Room temperature liquefied petroleum gas (LPG) sensor based on ppolyaniline/n-TiO2 heterojunction, Sens. Actuators, B134 (2008) 988–992.

[127] D.S. Dhawale, D.P. Dubal, V.S. Jamadade, R.R. Salunkhe, S.S. Joshi, C.D. Lokhande, Room temperature LPG sensor based on n-CdS/p-polyaniline heterojunction, Sens. Actuators, B145 (2010) 205–210.

[128] D.S. Dhawale, R.R. Salunkhe, U.M. Patil, K.V. Gurav, A.M. More, C.D. Lokhande, Room temperature liquefied petroleum gas (LPG) sensor based on p-polyaniline/n-TiO2 heterojunction, Sensors and Actuators B 134 (2008) 988–992

[129] T. Sen, N.G. Shimpi, S. Mishra, R.P. Sharma, Polyaniline/g-Fe_2O_3 nanocomposite for room temperature LPG sensing, Sens. Actuators, B, 190 (2014)120–126.

[130] B.A. Bhanvase, N.S. Darda, N.C. Veerkar, A.S. Shende, S.R. Satpute, S.H. Sonawane, Ultrasound assisted synthesis of PANI/ZnMoO4 nanocomposite for simultaneous improvement in anticorrosion, physico-chemical properties and its application in gas sensing Ultrasonics Sonochemistry 24 (2015) 87–97.

[131] P.T. Patil, R.S. Anwane, S.B. Kondawar, Development of electrospun polyaniline/ZnO composite nanofibers for LPG sensing Procedia Materials Science 10 (2015) 195 – 204.

[132] Y. Ali, V. Kumar, R.G. Sonkawade, A. S. Dhaliwal, Fabrication of polyaniline nanofibers by chronopotentiometery, Adv. Mat. Lett. 3(2012) 388-392.

[133] Y Ali, V. Kumar, A.S. Dhaliwal, R.G. Sonkawade, Surface modification of polyaniline nanofiber using silver nanoparticles to enhance sensing properties, Adv. Mat. Lett. 4(2013), 368-372.

[134] Y. Ali, V Kumar, R.G. Sonkawade, A.S. Dhaliwal, Effect of swift heavy ion beam irradiation on Au-polyaniline composite films, Vacuum 90 (2013) 59-64

[135] Y Ali, V Kumar, R.G. Sonkawade, M.D. Shirsat, A.S. Dhaliwal, Two-step electrochemical synthesis of Au nanoparticles decorated polyaniline nanofiber, Vacuum 93 (2013) 79-83

[136] S.B. Kadam, K. Datta, P. Ghosh, A.B. Kadam, P.W. Khirade, V. Kumar, R.G. Sonkawade, A.B. Gambhire, M.K. Lande, M.D. Shirsat, Improvement of ammonia sensing properties of poly(pyrrole)–poly (n-methylpyrrole) composite by ion irradiation, Appl Phys A 100 (2010) 1083–1088.

[137] B.S. Khened, T. Machappa, M.V.N. Pradeep, M.V.N. Ambika Prasad, M. Sasikala, Studies on LPG Sensing Property of Polyaniline / BaZrO3 Composites, Materials Today: Proceedings 3 (2016) 369 – 375

[138] S.S. Joshi, T.P. Gujar, V.R. Shinde, C.D. Lokhande, Fabrication of *n*-CdTe/*p*-polyaniline heterojunction-based room temperature LPG sensor, Sensors and Actuators B 132 (2008) 349–355

[139] T. Sen, N. G. Shimpi, S. Mishra, R. Sharma, Polyaniline/Fe2O3 nanocomposite for room temperature LPG sensing, Sensors and Actuators B 190 (2014) 120– 126

[140] N.M. Shinde, P.R. Deshmukh, S.V. Patil, C.D. Lokhande, Development of polyaniline/Cu2ZnSnS4 (CZTS) thin film based heterostructure as room temperature LPG sensor, Sensors and Actuators A 193 (2013) 79– 86.

[141] K. Nemade, S. Waghuley, Study of Cerium Doped Polyaniline Composites for Resistive Type CO_2 Gas Detection, Walailak J Sci & Tech 11 (2014)763-767.

[142] S.H. Nimkar, S.B. Kondawar, P.S. More, Polyaniline/TiO_2 Nanocomposite Thin Film Based Carbon Dioxide Gas Sensor, International journal of research in biosciences, agriculture and technology, (2015)12-18.

[143] M.K. Ram, Ö. Yavuz, V. Lahsangah, M. Aldissi, CO gas sensing from ultrathin nano-composite conducting polymer film, Sens. Actuators B Chem. 106 (2005) 750–757

[144] B.L. Risavi, R.J. Wadas Jr., C. Thomas, D.F. Kupas, A novel method for continuous environmental surveillance for carbon monoxide exposure to protect emergency medical service providers and patients, J. Emerg. Med. 44 (2013) 637–640

[145] T. Zhang, L. Liu, Q. Qi, S. Li, G. Lu, Development of microstructure In/Pd-doped SnO_2 sensor for low-level CO detection, Sens. Actuators B: Chem. 139 (2009) 287–291.

[146] S.C.K. Mishra, P. Mathur, B.K. Srivastava, Vacuum-deposited nanocrystalline polyaniline thin film sensors for detection of carbon monoxide. Sens. Actuators, A 114 (2004) 30–35.

[147] N. Densakulprasert, L. Wannatong, D. Chotpattananont, P. Hiamtup, A. Sirivat, J. Schwank, Electrical Conductivity of Polyaniline/Zeolite Composites and Synergetic Interaction with CO. Mater. Sci. Eng., B 117 (2005) 276–282.

[148] T. Sen, N.G. Shimpi, S. Mishra, Room temperature CO sensing by polyaniline/Co_3O_4 nanocomposite, Journal of applied and polymer science, J. Appl. Polym. Sci. 133 (2016) 44115.

[149] S. Das, S. Chakraborty, O. Parkash, D. Kumar, S. Bandyopadhyay, S. K. Samudrala, A. Sen, H. S. Maiti, Vanadium doped tin dioxide as a novel sulfur dioxide sensor, Talanta, 75 (2008) 385–389.

[150] S. C. Lee, B. W. Hwang, S. J. Lee, H. Y. Choi, S. Y. Kim, S. Y. Jung, D. Ragupathy, D. D. Lee, J. C. Kim, A novel tin oxide-based recoverable thick film SO_2 gas sensor promoted with magnesium and vanadium oxides, Sens. Actuators, B160 (2011) 1328–1334.

[151] K. Wetchakun, T. Samerjai, N. Tamaekong, C. Liewhiran, C. Siriwong, V. Kruefu, A. Wisitsoraat, A. Tuantranont, S. Phanichphant, Semiconducting metal oxides as sensors for environmentally hazardous gases, Sens. Actuators, B160 (2011) 580–591.

[152] M. Matsuguchi, K. Tamai, Y. Sakai, SO_2 gas sensors using polymers with different amino groups, Sens. Actuators, B 77 (2001) 363–367.

[153] P. Kiattibutr, L. Tarachiwin, L. Ruangchuay, A. Sirivat, J. Schwank, React. Funct. Polym. Electrical conductivity responses of polyaniline films to SO_2-N_2 mixtures: Effect of dopant type and doping level, 53 (2002) 29–37.

[154] N. E. Agbor, M. C. Petty and A. P. Monkman, Polyaniline thin films for gas sensing, Sens. Actuators, B28 (1995) 173–179.

[155] J. Sarfraz, P. Ihalainen, A. M¨a¨att¨anen, J. Peltonen and M. Lind´en, Printed hydrogen sulfide gas sensor on paper substrate based on polyaniline composite, Thin Solid Films, 534 (2013) 621–628.

[156] W. P. Jakubik, M. Urbanczyk, E. Maciak, T. Pustelny, A. Stolarczyk, Polyaniline thin films as a toxic gas sensors in saw system, Molecular and Quantum Acoustics, 28 (2007) 125–129.

[157] P. S. Barker, C. D. Bartolomeo, A. P. Monkman, M. C. Petty, R. Pride, Gas sensing using a charge-flow transistor, Sens. Actuators, B 24–25 (1995) 451–453.

[158] A. Boudiba, C. Zhang, C. Bittencourt, P. Umek, M. Olivier, R. Snyders, M. Debliquy, SO_2 Gas Sensors based on WO_3 Nanostructures with Different Morphologies, Procedia Eng., 47 (2012) 1033– 1036.

[159] Y. Shimizu, N. Matsunaga, T. Hyodo, M. Egashira, Improvement of SO_2 sensing properties of WO_3 by noble metal loading, Sens. Actuators, B 77 (2001) 35–40.

[160] N. Izu, G. Hagen, D. Sch¨onauer, U. R¨oder-Roith, R. Moos, Application of $V_2O_5/WO_3/TiO_2$ for Resistive-Type SO_2 Sensors, Sensors, 11 (2011) 2982–2991.

[161] M. Penza, G. Cassano, F. Tortorella, Gas recognition by activated WO_3 thin-film sensors array, Sens. Actuators, B 81 (2000) 115–121.

[162] C.A. Betty, S. Choudhury, S. Arora, Tin oxide–polyaniline heterostructure sensors for highly sensitive and selective detection of toxic gases at room temperature, Sensors and Actuators B 220 (2015) 288–294.

[163] V. Chaudhary, A. Kaur, Enhanced room temperature sulfur dioxide sensing behaviour of in situ polymerized polyaniline– tungsten oxide nanocomposite possessing honeycomb morphology. RSC Adv., 5 (2015) 73535.

[164] Y. X. Gan , R. H. Yazawa, J. L. Smith , J. C. Oxley , G. Zhang , J. Canino , J. Ying, G. Kagan, L. Zhang, Nitroaromatic explosive sorption and sensing using electrochemically processed polyaniline-titanium dioxide hybrid nanocomposite, Materials Chemistry and Physics 143 (2014) 1431-1439.

[165] S. H. Hosseini, Investigation of Sensing Effects of Polystyrene-graft Polyaniline for Cyanide Compounds, Journal of Applied Polymer Science, 101 (2006) 3920 – 3926.

[166] S. Virji, R. Kojima, J. D. Fowler, R. B. Kaner, B. H. Weiller, Polyaniline Nanofiber-Metal Salt Composite Materials for Arsine Detection, Chem. Mater. 21 (2009) 3056–3061.

[167] F. Worek, M. Koller, H. Thiermann, L. Szinicz, Diagnostic aspects of organophosphate poisoning, Toxicology 214 (2005) 182–189.

[168] C.-P. Chang, C.-L. Yuan, The fabrication of a MWNTs–polymer composite chemoresistive sensor array to discriminate between chemical toxic agents, J. Mater. Sci. 44 (2009) 5485–5493.

[169] R. Yoo, J. Kim, M-J. Song, W. Lee, J. S. Noh, Nano-composite sensors composed of single-walled carbon nanotubes and polyaniline for the detection of a nerve agent simulant gas , Sensors and Actuators B 209 (2015) 444–448.

[170] C-L. Yuan, C-P. Chang, MWNTs/Polyaniline Composite Chemoresistive Sensor Array for Chemical Toxic Agents Detection, Journal of Chung Cheng Institute of Technology 38(2009) 147-156

[171]Centers for Disease Control and Prevention. http://www.bt.cdc.gov/agent/phosgene/basics/facts.asp (accessed Aug. 29, 2008).

[172] S. Virji, R. Kojima, J.D. Fowler, J. G. Villanueva, R. B. Kaner , B. H. Weiller, Polyaniline Nanofiber Composites with Amines: Novel Materials for Phosgene Detection, Nano Res 2 (2009) 135 142.

[173] H. Babad, A.G. Zeiler, Chemistry of phosgene. Chem. Rev. 73 (1973)75- 91.

[174] Y.S. Jung, W. Jung, H.L. Tuller, C.A Ross. Nanowire Conductive Polymer Gas Sensor Patterned Using Self- Assembled Block Copolymer Lithography. Nano Letters 8(2008) 3776-80.

List of figures and table caption

Figure 1 This scheme shows two different emeraldine class of PANI (a) non-conducting emeraldine base form of PANI. (b) Conducting emeraldine salt form of PANI.

Figure 2 Illustrates the PANI-based nanocomposite used to detect gasses for sensing applications.

Figure 3. Schematic representation of the sensor testing setup.

Figure 4. Schematic diagram of the formation of SnO_2/PANI nanocomposite thin films. [Reprinted with permission from ref 36. Copyright 2009 Elsevier].

Figure 5. *I–V* curves (in the presence of NH_3 gas) for (a) SnO_2, (b) PANI and (c) SnO_2/PANI nanocomposites. [Reprinted with permission from ref 36. Copyright 2009 Elsevier].

Figure 6. Schematic showing the synthesis of PANI functionalized MWCNTs.

Figure 7. SEM images of cellulose (a), cellulose/TiO_2 (b), cellulose/PANI (c) and cellulose/TiO_2/PANI composite nanofibers (d). [Reprinted with permission from ref 49. Copyright 2016 Elsevier].

Figure. 8. Schematic diagram for the synthesis of S, N: GQDs **(a);** Schematic diagram of gas sensor fabrication process of sensing devices based on S, N: GQDs/PANI hybrids **(b).** [Reprinted with permission from ref 58. Copyright 2016 Elsevier].

Figure. 9 Response versus time plot for unirradiated and Irradiated Ta/PANI composite sensors after hydrogen exposure at RT. [Reprinted with permission from ref 67. Copyright 2012 Elsevier].

Figure. 10. The schematic block diagram of our handmade hydrogen gas sensing setup. [Reprinted with permission from ref 70. Copyright 2015 Elsevier].

Figure. 11. Sensing performance of Sensor S5P500 and S5P100 at 140°C over a longer working time period. The target gas is NO_2 with a concentration of 37 ppm. [Reprinted with permission from ref 104. Copyright 2016 Elsevier].

Figure. 12. Gas responses of PANI–CdS nanocomposite sensor film to 20 ppm of H_2S and 100 ppm of CH_3–OH, C_2H_5–OH, NO_2 and NH_3 [Reprinted with permission from ref 108. Copyright 2012 Elsevier].

Figure. 13. (a) A schematic of an SWCNT–polyaniline composite sensor on an oxidized Si substrate with Pd electrodes. The inset shows an SEM image of the SWCNT–polyanilinecomposite. (b and c) TEM images of SWCNTs–polyaniline composite. [Reprinted with permission from ref 169. Copyright 2015 Elsevier].

Figure. 14. (a) Real-time response curves as a function of DMMP concentration at room temperature and (b) response versus DMMP concentration. [Reprinted with permission from ref 169. Copyright 2015 Elsevier].

Table 1 Sensor response (S), response time (t_{res}), recovery time (t_{rec}), studied detection range (DR), PANI based nanocomposite material (M) and operating temperature (T) of the various gas sensors.

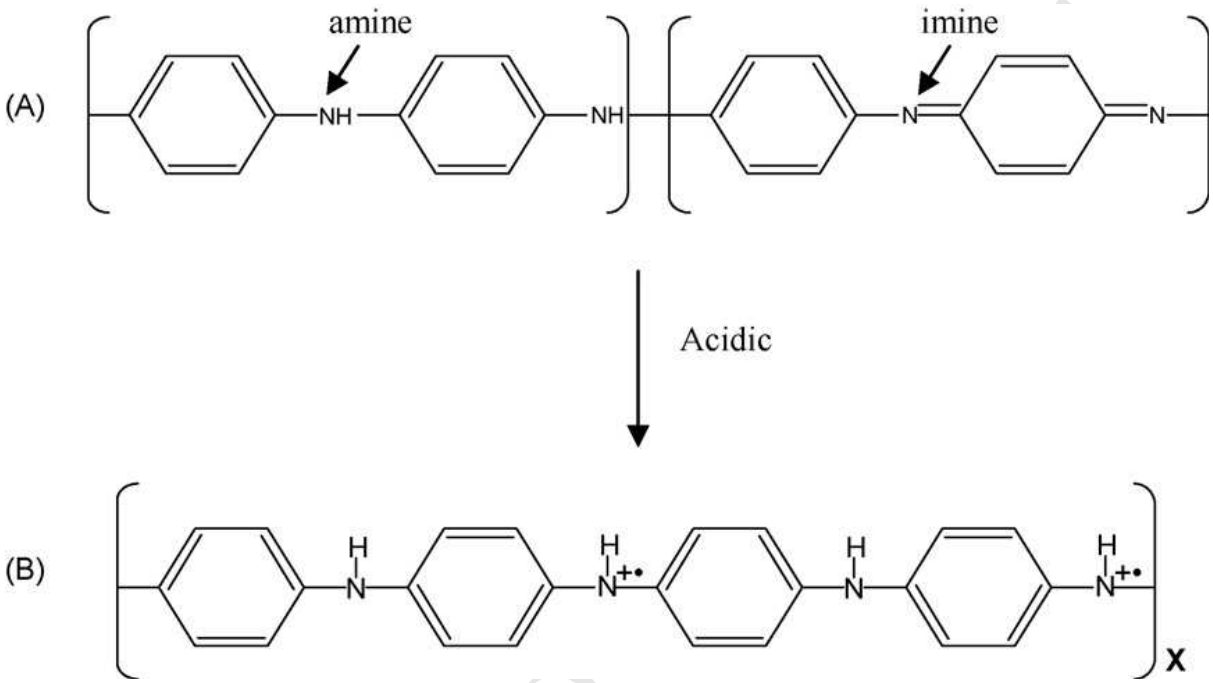

Figure 1

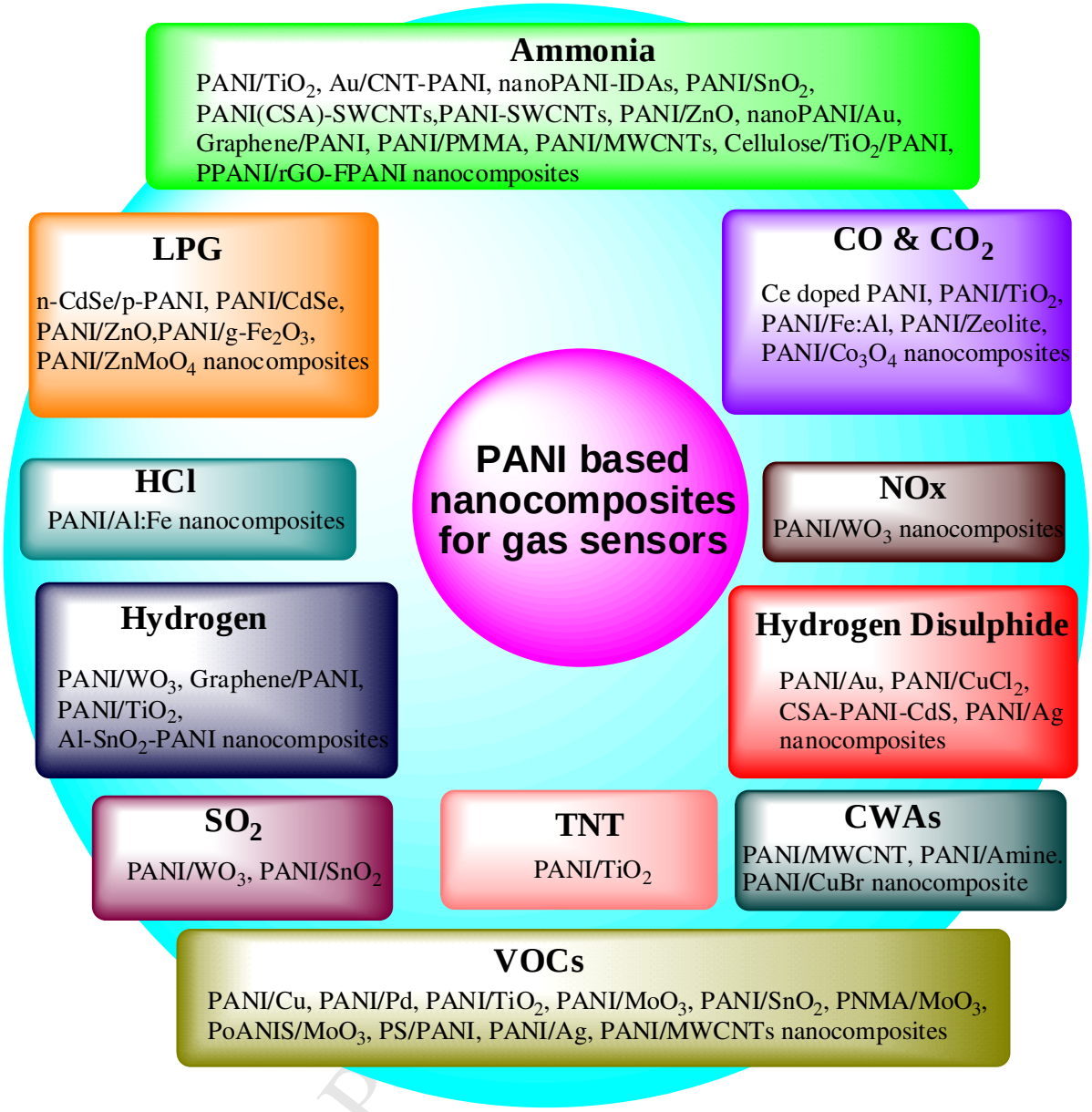
Ammonia
PANI/TiO2, Au/CNT-PANI, nanoPANI-IDAs, PANI/SnO2, PANI(CSA)-SWCNTs,PANI-SWCNTs, PANI/ZnO, nanoPANI/Au, Graphene/PANI, PANI/PMMA, PANI/MWCNTs, Cellulose/TiO2/PANI, PPANI/rGO-FPANI nanocomposites
LPG
n-CdSe/p-PANI, PANI/CdSe, PANI/ZnO,PANI/g-Fe2O3, PANI/ZnMoO4 nanocomposites
CO & CO2
Ce doped PANI, PANI/TiO2, PANI/Fe:Al, PANI/Zeolite, PANI/Co3O4 nanocomposites
PANI based nanocomposites for gas sensors
HCl
PANI/Al:Fe nanocomposites
NOx
PANI/WO3 nanocomposites
Hydrogen
PANI/WO3, Graphene/PANI, PANI/TiO2, Al-SnO2-PANI nanocomposites
Hydrogen Disulphide
PANI/Au, PANI/CuCl2, CSA-PANI-CdS, PANI/Ag nanocomposites
SO2
PANI/WO3, PANI/SnO2
TNT
PANI/TiO2
CWAs
PANI/MWCNT, PANI/Amine. PANI/CuBr nanocomposite
VOCs
PANI/Cu, PANI/Pd, PANI/TiO2, PANI/MoO3, PANI/SnO2, PNMA/MoO3, PoANIS/MoO3, PS/PANI, PANI/Ag, PANI/MWCNTs nanocomposites

Figure 2

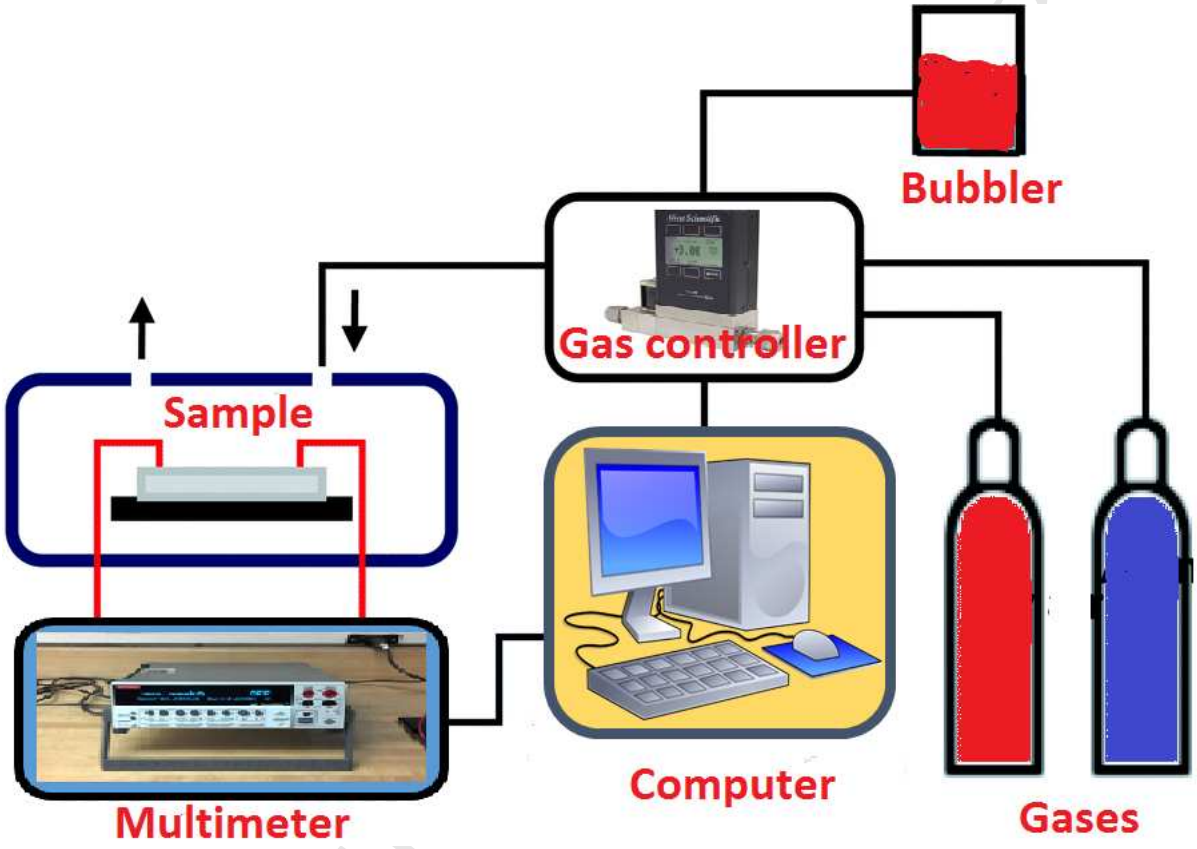

Figure 3

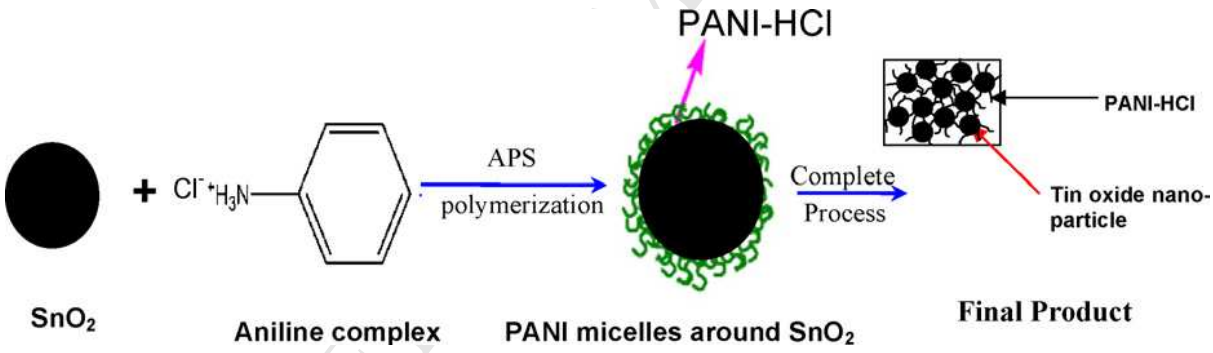

Figure 4

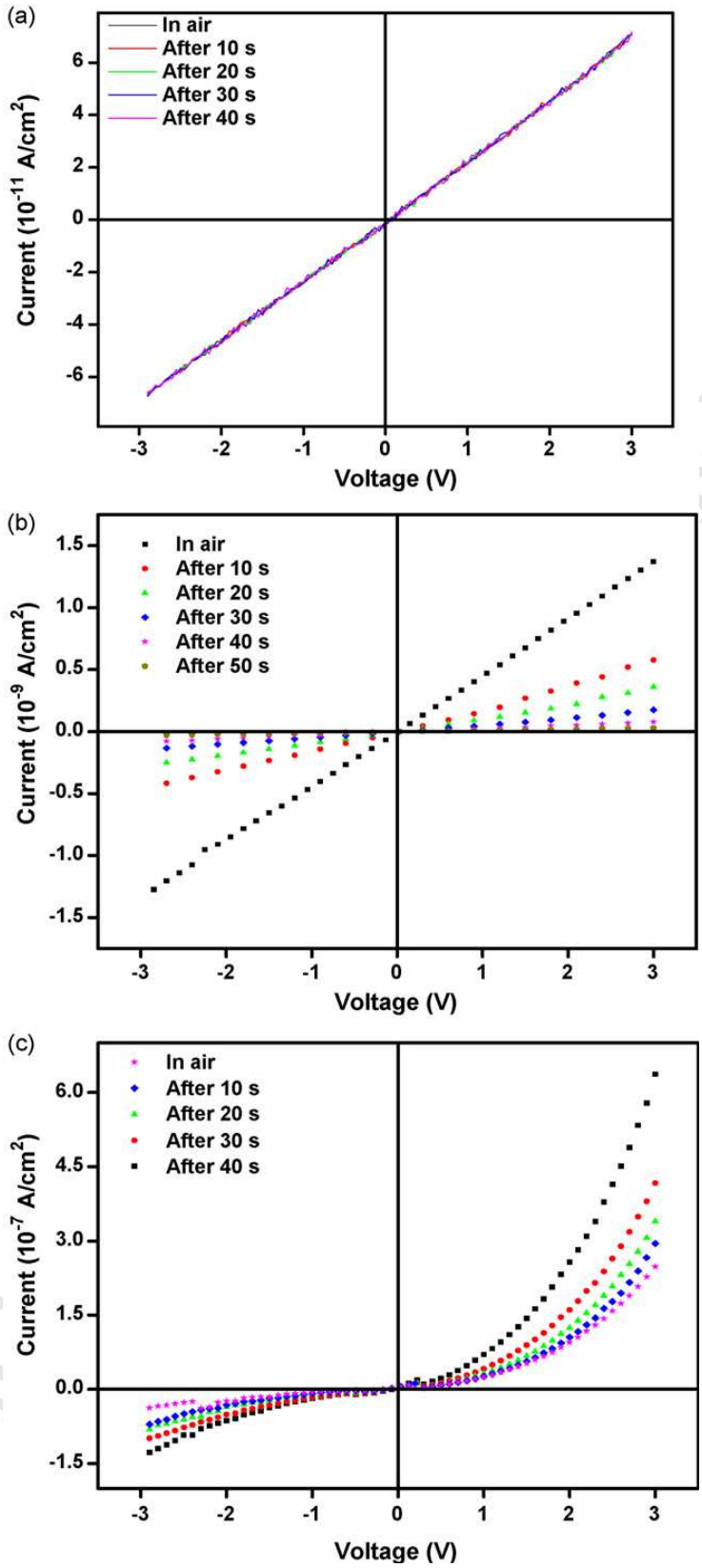
(a)
In air
After 10 s
After 20 s
After 30 s
After 40 s
Current (10^{-11} A/cm^2)
Voltage (V)
(b)
In air
After 10 s
After 20 s
After 30 s
After 40 s
After 50 s
Current (10^{-9} A/cm^2)
Voltage (V)
(c)
In air
After 10 s
After 20 s
After 30 s
After 40 s
Current (10^{-7} A/cm^2)
Voltage (V)

Figure 5

1718

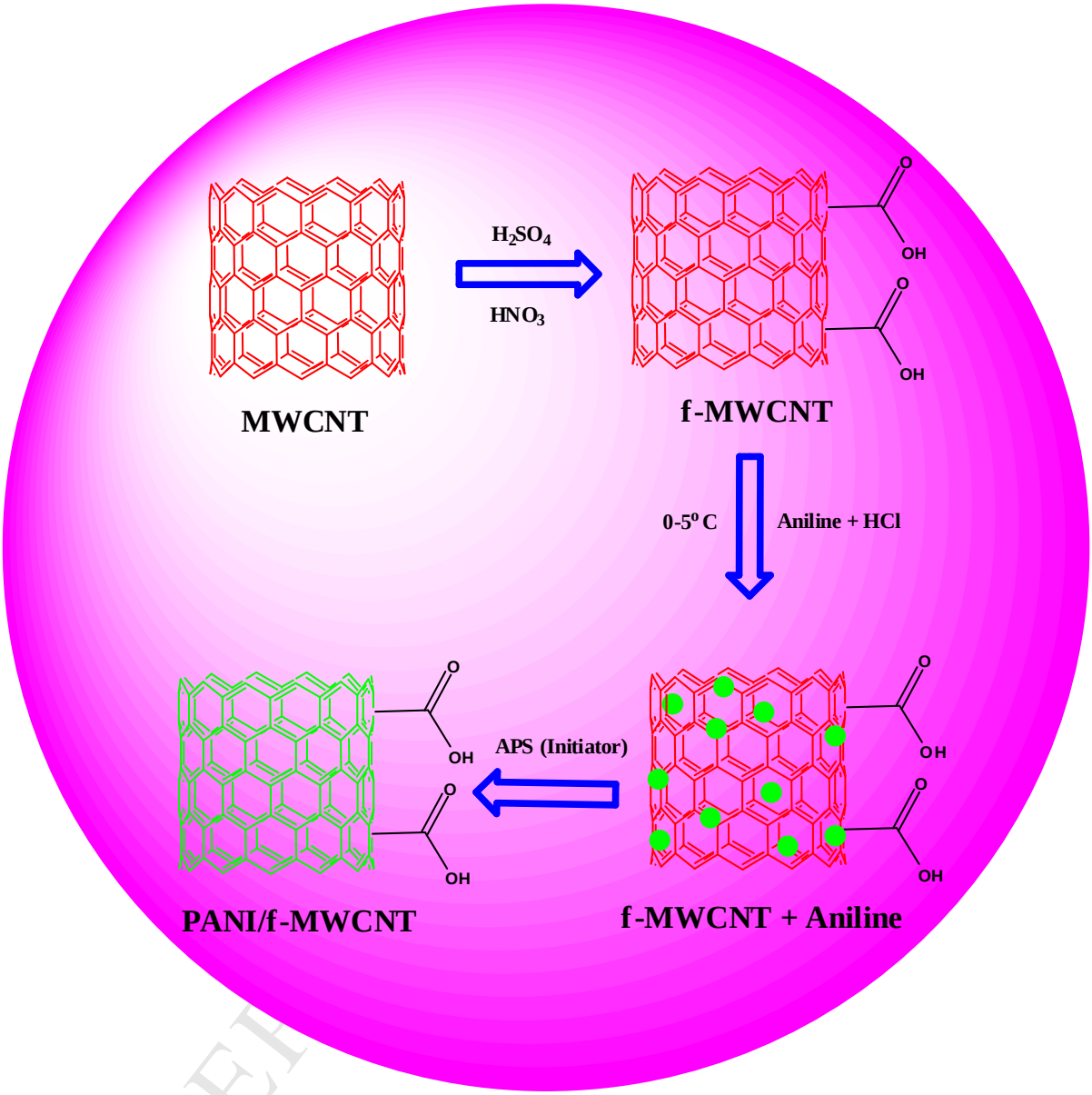

1719
1720

1721 **Figure 6.**

1722

1723

1724

1725

1726

1727

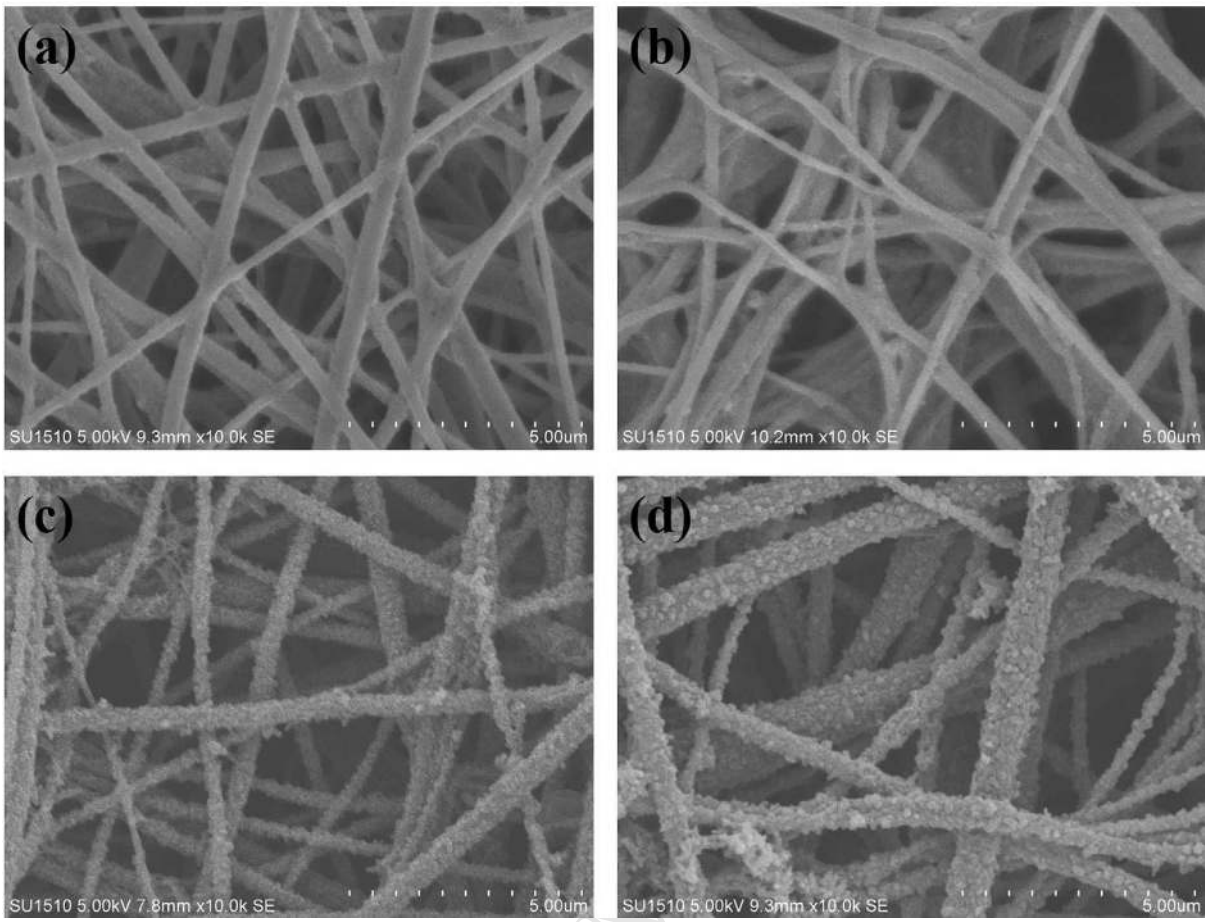

Figure 7.

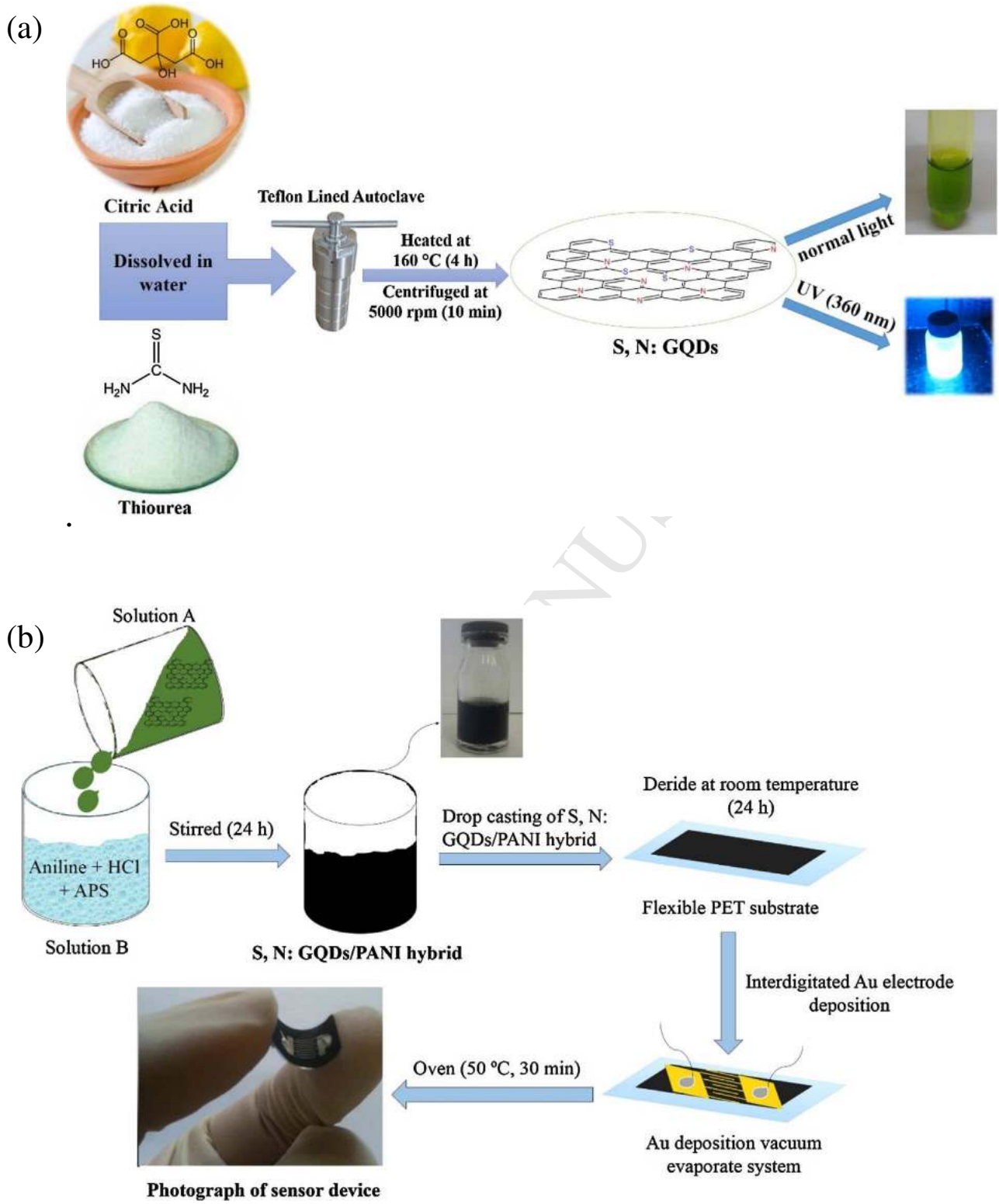
(a)
Citric Acid
Dissolved in water
Teflon Lined Autoclave
Heated at 160 °C (4 h)
Centrifuged at 5000 rpm (10 min)
S, N: GQDs
normal light
UV (360 nm)
Thiourea
(b)
Solution A
Aniline + HCl + APS
Solution B
Stirred (24 h)
S, N: GQDs/PANI hybrid
Drop casting of S, N: GQDs/PANI hybrid
Deride at room temperature (24 h)
Flexible PET substrate
Interdigitated Au electrode deposition
Au deposition vacuum evaporate system
Oven (50 °C, 30 min)
Photograph of sensor device

Figure. 8

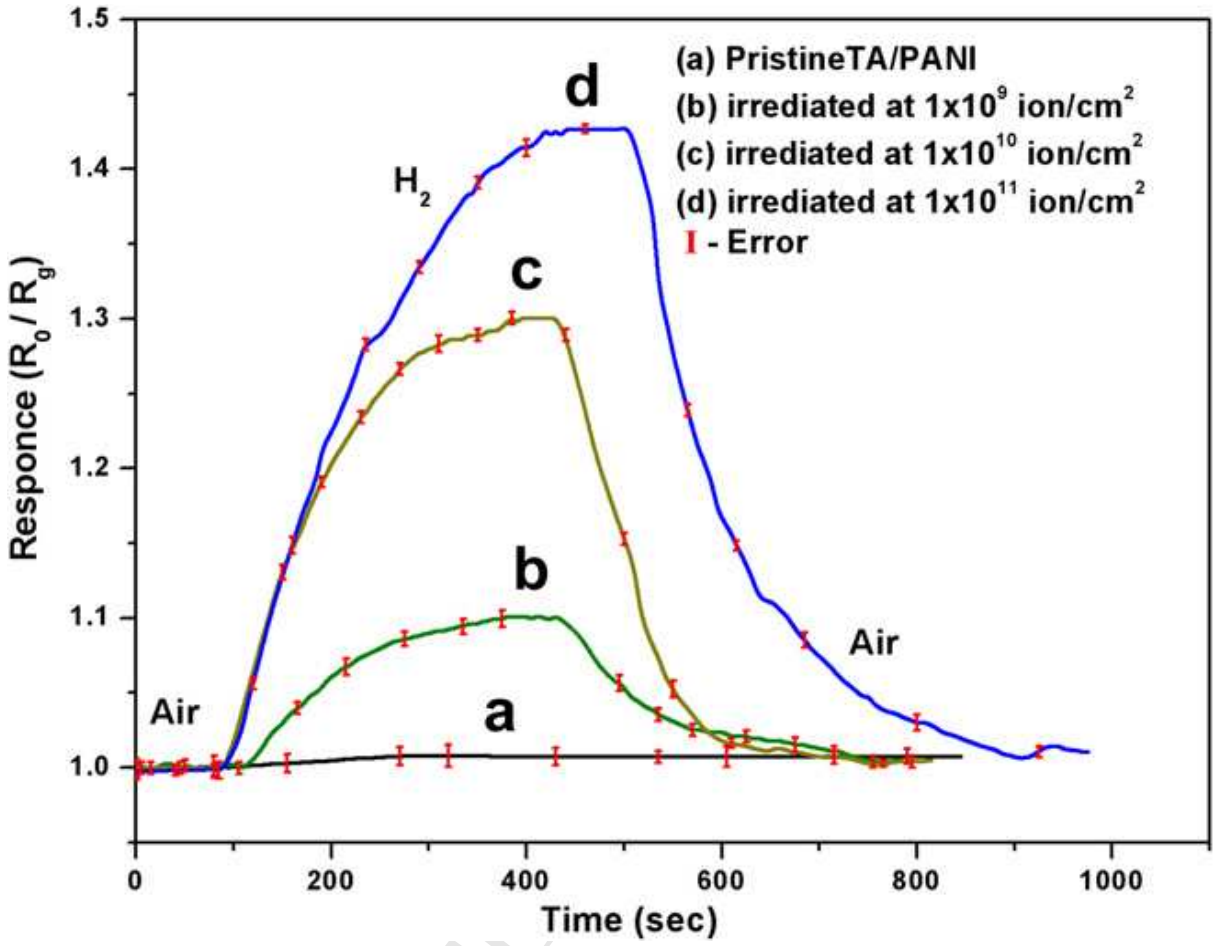
(a) PristineTA/PANI
(b) irrediated at 1x10^9 ion/cm^2
(c) irrediated at 1x10^10 ion/cm^2
(d) irrediated at 1x10^11 ion/cm^2
I - Error
d
c
b
a
H2
Air
Air
Responce (R0 / Rg)
Time (sec)
1.0
1.1
1.2
1.3
1.4
1.5
0
200
400
600
800
1000

Figure. 9

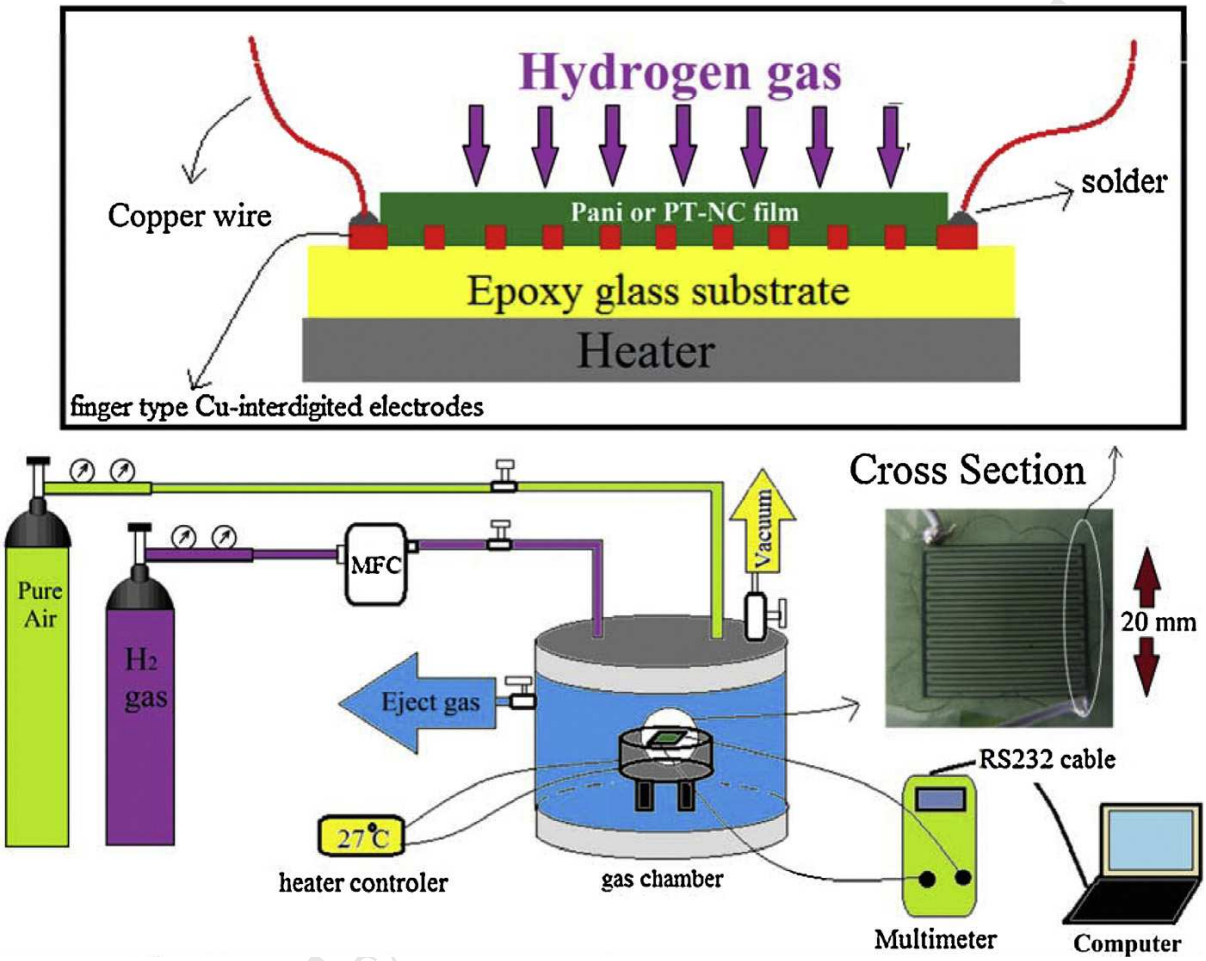
Hydrogen gas
Copper wire
Pani or PT-NC film
solder
Epoxy glass substrate
Heater
finger type Cu-interdigited electrodes
Cross Section
Pure Air
H2 gas
MFC
Vacuum
Eject gas
20 mm
RS232 cable
27℃
heater controler
gas chamber
Multimeter
Computer

Figure. 10.

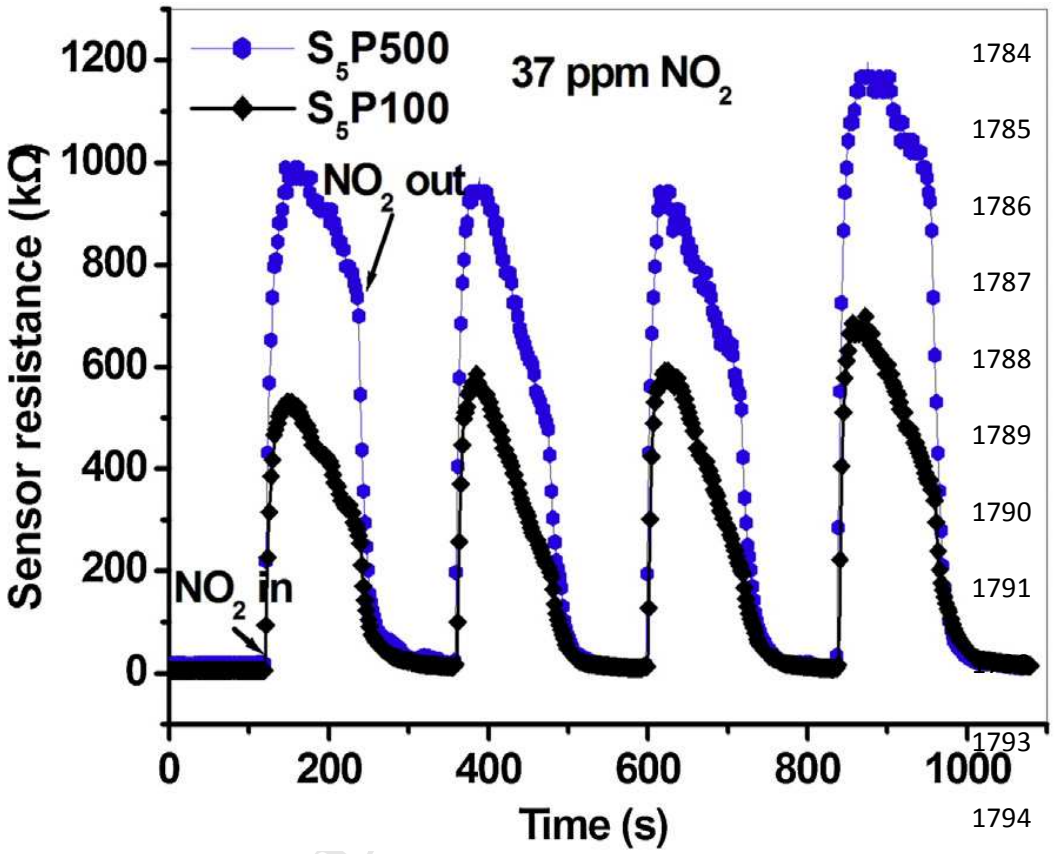
S5P500
S5P100
37 ppm NO2
NO2 out
NO2 in
Sensor resistance (kΩ)
Time (s)
0
200
400
600
800
1000
1200

Figure. 11

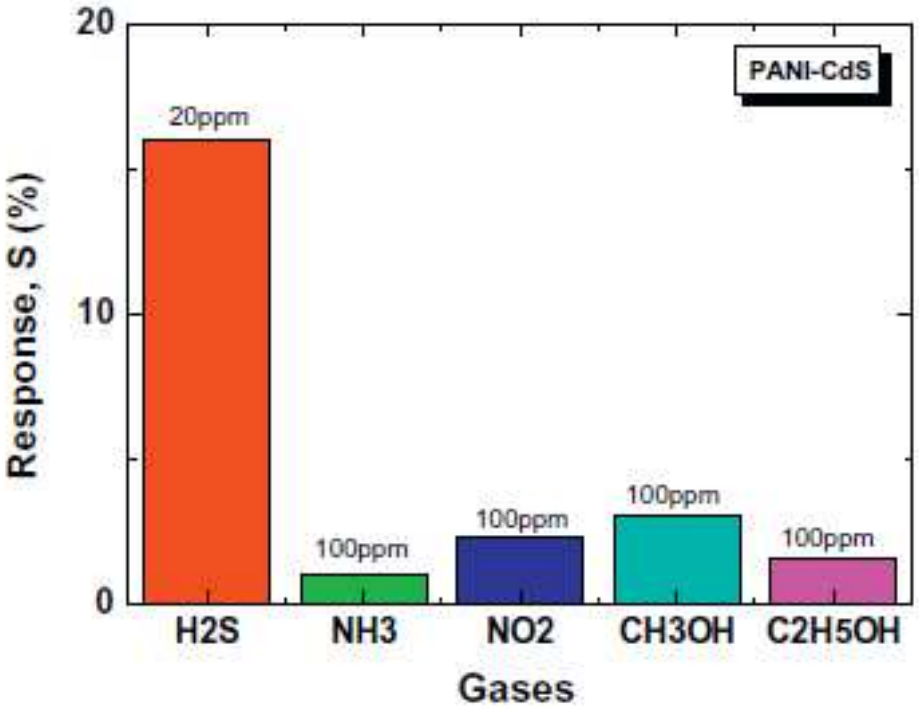
20
10
0
Response, S (%)
PANI-CdS
20ppm
100ppm
100ppm
100ppm
100ppm
H2S
NH3
NO2
CH3OH
C2H5OH
Gases

Figure. 12.

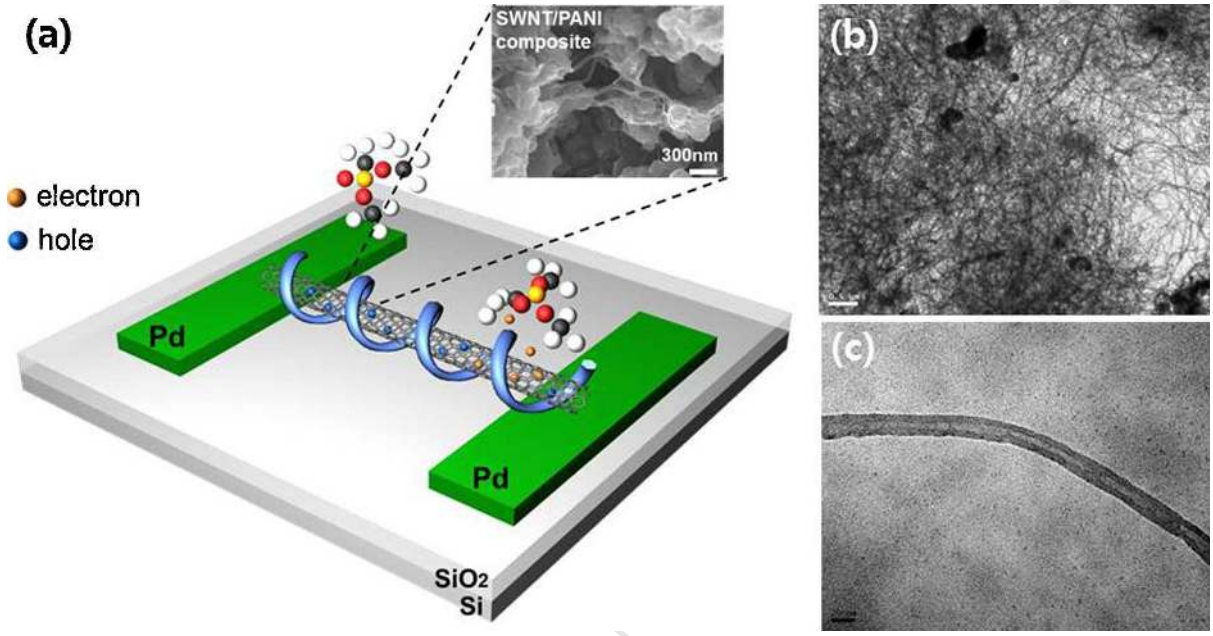

Figure. 13.

1835

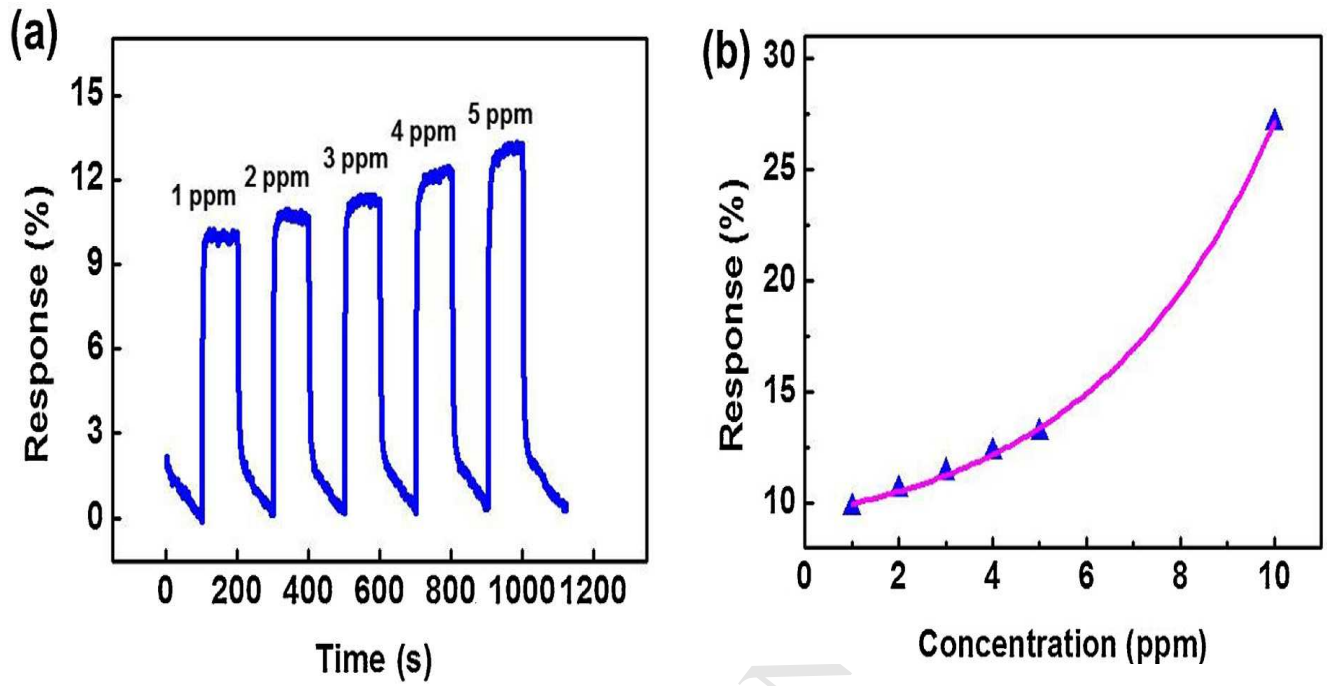

1836

1837

1838

1839

1840 **Figure. 14.**

1841

1842

1843

1844

1845

1846

1847

1848

1849

1850 **Table 1** Sensor response (S), response time (t_{res}), recovery time (t_{rec}), studied detection range
1851 (DR), PANI based nanocomposite material (M) and operating temperature (T) of the various
1852 gas sensors.

M	S (%)	t_{res} (sec)	t_{rec} (sec)	D_R	T (°C)	Reference
Ammonia (NH_3) Detection						
PANI nanobowl-AuNPs (15 nm)	3.2 (100 ppm)	5	7	0-1600 ppm	RT	[22]
PANI/TiO_2	1.67 (23 ppm), 5.55 (117 ppm)	18	58	23–141 ppm	25°C	[33]
Au/CNT-PANI	0.638 (25 ppm)	600	900	200 ppb-10 ppm	RT	[34]
NanoPANI-IDAs	0.24 (100 ppm)	90	90	1-100 ppm	RT	[35]
SnO_2/PANI	16 (500 ppm)	12-15	80	100–500 ppm	RT	[36]
PANI(CSA)–SWNTs	50 (400 ppm at 0% RH)	-	-	10 ppb-400 ppm	24°C	[37]
PANI/TiO_2, PANI/SnO_2 and PANI/In_2O_3	PANI/TiO_2 (1.5 for 23 ppm and 9 for 141 ppm); PANI/SnO_2(1.2 for 23 ppm and 7 for 141 ppm); PANI/In_2O_3 (0.45 for 23 ppm and 1.35	>10	>60	23-141 ppm	RT	[38]

	for 141 ppm)					
PANI–SWNTs	5.8 (50 ppb)	450	-	25-200 ppb	RT	[39]
TiO_2 microfibers enchased with PANI nanograins	0.004 (50 ppt)	~100	-	50-200 ppt	RT	[40]
PANI/TiO_2	12 (20 ppm)	72		340 s	RT	[41]
Core-shell PANI	0.11 (1 ppm)	150	300	20 ppb to 10 ppm	25°C	[42]
PANI-ZnO (50 %)	~ 4.6(20 ppm)	153	135	20 to 100 ppm	-	[43]
Graphene/PANI	3.65 (20 ppm), 11.33 (100 ppm)	50	23	1–6400 ppm	25°C	[46]
MWCNT/PANI	15.5	6	35	2 ppm	25°C	[48]
(cellulose/TiO_2/PANI) composite	6.3 (250 ppm)			10-250ppm	RT	[49]
(PPANI/rGO-FPANI) nanocomposite	~5 (10 ppm)	36	18	100 ppb to 100 ppm	12–40 °C	[50]
PANI/NiTSPc composite	0.60 (5 ppm), 2.75 (100 ppm)	10	46	5–2500	25°C	[51]
CSA doped PANI-SnO_2	0.91 (100 ppm)	46	3245	10–100	30°C	[54]
Si/PANI	0.8 (20 ppm) 1.7 (90 ppm)	25s	360s	10–90	25°C	[55]
pf-MWCNT/PANI	0.015 (20 ppm), 0.075 (100 ppm)	100	700	0–100	25°C	[56]

S, N: GQDs/PANI hybrid	42.3 (100 ppm), 385 (1000 ppm)	115	44	1–1000	25°C	[58]
Hydrogen (H_2) Detection						
graphene/PANI nanocomposite	16.57(1% H_2)	-	-	-	24°C	[63]
Polyaniline (emeraldine)/anatase TiO_2 nanocomposite	1.63 (0.8% H_2)	83	130	-	RT	[64]
Al-SnO_2/PANI composite nanofibers	~275 (1000ppm)	2	2	-	48˚C	[65]
CNT doped PANI	1.07 (2%)	-	-	-	RT	[66]
Ta/PANI	1.42	-	-	-	RT	[67]
PANI/TiO_2:SnO_2	1.25 (0.8% H_2)	75	117		27°C	[70]
Chitosan/PANI composite	130 (4% H_2)			0.3% - 4%	RT	[94]
Hydrochloric Acid (HCl) Detection						
HCHO/PANI composite	800 (20 ppm)	10	-	0.01 to 100 ppm	RT	[98]
Nitrogen oxides (NO_2) Detection						
PANI/MWCNT/TiO_2	23.5 (25 ppm)	-	-	-	22°C	[99]
SnO_2–ZnO (20 wt %)/PANI	368.9 (35 ppm)	9s	27s	-	180°C	[100]
1% PANI)-SnO_2 sensor	3.01×10^2 (10 ppm)	-	-	-	40°C	[103]
SnO_2/PANI	4 (37ppm)	17	25	5-55 ppm	140°C	[104]

Hydrogen Disulfide (H_2S) Detection						
CSA-doped PANI-CdS	76 (100 ppm)	-	413s	10-100 ppm	RT	[107]
PANI–CdS	~48 (100 ppm)	~41-71s	~345 - 518s	-	RT	[108]
Flexible PANI–Ag	100 (10 ppm)	360s		1-25 ppm	RT	[109]
Volatile Organic Compounds (VOCs) Detection						
Chloroform ($CHCl_3$) detection						
PANI/Cu nanocomposite	1.5 (10 ppm)	-	-	10-100ppm	-	[25]
Methanol (CH_3OH) detection						
PANI/Pd nanocomposite	104 (2000ppm)	-	-	-	RT	[27]
Trimethylamine $(CH_3)_3N$ detection						
PANI/TiO_2	5.14 X 10-7 ML^{-1}	180	-	-	RT	[115]
Formaldehyde (HCHO) detection						
(PANI) x MoO_3, on $LaAlO_3$(100) (LAO) substrate.	8 (50 ppm)	600	-	-	30°C	[116]
(PoANIS)xMoO_3 thin films	6 (25-400ppb)	-	-	25-400 ppb	30°C	[119]
Aromatic hydrocarbon detection						
PANI-MWCNT (mass ratio 4:1)	0.31 (1000 ppm)	-	-	200-1000	RT	[122]

				ppm		
Liquefied petroleum gas (LPG) Detection						
PANI/TiO_2	63 (0.1 vol %)	-	-	-	RT	[125]
PANI/CdSe	80 (1040 ppm)	-	-	-	RT	[126]
PANI/ZnO	81 (1040 ppm)	-	-	-	RT	[127]
p-PANI/n-TiO_2	63 (0.1 vol%)	140		(0.02-0.1vol %)	RT	[128]
PANI/g-Fe_2O_3	1.3 (200 ppm)				RT	[129]
PANI/$ZnMoO_4$	20.6-45.8 (800-1800ppm)	600	840	(800-1800 ppm)	RT	[130]
PANI/ZnO	7.33 (1000 ppm)	100	185		RT	[131]
n-CdTe/p-PANI	67.7 (0.14 vol%)	80-300	600	(0.02-0.14 vol%)	RT	[138]
PANI/Fe_2O_3	0.5 (50 ppm)	60		(50-200 ppm)	RT	[139]
PANI/Cu_2ZnSnS_4	44 (0.06 vol%)	-	-	-	RT	[140]
CO_2 Detection						
PANI/TiO_2	5 (1000 ppm)	70	80	-	35°C	[142]
CO Detection						
PANI/Fe:Al (80:20)	400 (0.006 ppm)	-	-	(0.006-0.3 ppm)	RT	[146]

PANI/Co_3O_4	0.81 (75 ppm)	40	-	-	RT	[148]
SO_2 Detection						
SnO_2–PANI heterostructure	2 ppm	-	-	-	25°C	[162]
PANI–WO_3 hybrid	10.6 (10 ppm)	-	-	5-80 ppm	30°C	[163]
Dimethyl-methyl-phosphonate (DMMP) Detection						
PANI/MWCNT	1 (332 ppm)	-	-	-	RT	[168]
PANI/SWCNT	27.1 (10 ppm)	5.5	-	-	RT	[169]

1853

1854

1855

1856

Highlights (for review)

- Recent review of new-generation polyaniline nanocomposite-based gas sensors.
- Polyaniline nanocomposites as resistive sensor are demonstrated.
- Several parameters including fabrication of sensors, linear ranges, limits of detection (LODs), and reproducibility are discussed in detail.
- PANI-based nanocomposite shows high selectivity, a fast response/recovery time and great stability.